POLITECNICO DI MILANO

Facoltà di Ingegneria dei Sistemi

Corso di laurea in Ingegneria Biomedica

Closed-loop neuroprosthesis for spinal cord injured patients

Relatore:

Prof.ssa Alessandra Pedrocchi

Correlatore:

Ing. Noelia Chia Bejarano

Elaborato di laurea di:

Riccardo Bellinetto 804290

Matteo Colombo 804467

Anno accademico 2015/2016

Index

Abstract

The term Spinal Cord Injury (SCI) refers to damage to the spinal cord resulting from trauma (e.g. a car crash) or from disease or degeneration (e.g. cancer) and it is defined as *an insult to the spinal cord resulting in a change, either temporary or permanent, in the cord's normal motor, sensory, or autonomic function* [1].

Incomplete spinal-cord injured subjects can benefit from neuro-motor rehabilitation. One of the most important rehabilitative treatment used to recover from neurological damages is Functional Electrical Stimulation (FES), and it is used, as proposed in different studies, to generate purposeful contractions of paralyzed muscles, thereby enabling functional activities such as cycling, standing and stepping. Besides, the muscular tone training, and the cardiovascular conditioning, FES has some effects on central nervous system circuits. In traversing spinal cord and ascending to the brain, the electrical stimulus increases activity in spinal and cortical circuits involved in the movement and this can lead to both short-term and long-term neuroplasticity [2] .

The main goal of this work was the implementation of a FES gait neuroprosthesis, for SCI subjects, based on data acquired from inertial and magnetic sensors, to control knee flexion and ankle dorsiflexion during the preparation and the beginning of the swing phase, and it was developed in collaboration with the CSIC laboratory in Madrid during the first three months. The implementation of the neuroprosthesis was divided in three main blocks: real-time detection of gait events, kinematic analysis and Iterative Learning Controller (ILC). The first block consisted in the optimization of an existing and validated algorithm for gait-event detection, through which the gait was segmented using thresholds automatically calculated during the calibration made with the first 4 steps of the subjects, and then updated step-by-step [3]. These processes were improved by separating the calibration from the real-time detection and the step-by-step update, allowing to have only one calibration during the first trial. The improved algorithm was validated analyzing the metrics Precision (P), Recall (R) and F1-score, computed as the harmonic mean between the other two metrics [3], on data

acquired during five different tasks (straight walking, changes in velocities, changes in slope, changes in direction, start and stop).

The results obtained show that precision, recall and F1-score, assumed high values during all the tasks performed, especially during straight walking at normal speed, in which no False Positive (FP) or False Negative (FN) were detected and so P, R and F1-score were equal to 1.

Through these changes in the algorithm, the gait events were detected from the first step and so the neuroprosthesis was able to work from the beginning of the trial.

The second block of the controller referred to the kinematic analysis, through which knee and ankle angles variations were extracted during walking. Three different algorithms were developed in order to reach this goal: the first was based on rotation matrices extracted from inertial and magnetic sensors, the second was based on integration of data acquired from accelerometers and gyroscopes and the third extracted the angles only from the gyroscopes, removing the eventual drift. The algorithms were validated on data collected from twelve subjects during rectilinear walking at normal speed. The third algorithm, based on "detrended" gyroscopes, provided the best results, and therefore it was chosen to extract knee and ankle angles in the final application.

The third block of the work referred to the implementation of an Iterative Learning Controller (ILC). The algorithm extracted the error between a pre-set reference trajectory and an online trajectory, calculated through kinematic analysis, during the preparation and the beginning of the swing phase, both for knee and ankle angles. If figure A is shown the flow diagram which describes the way in which the controller works

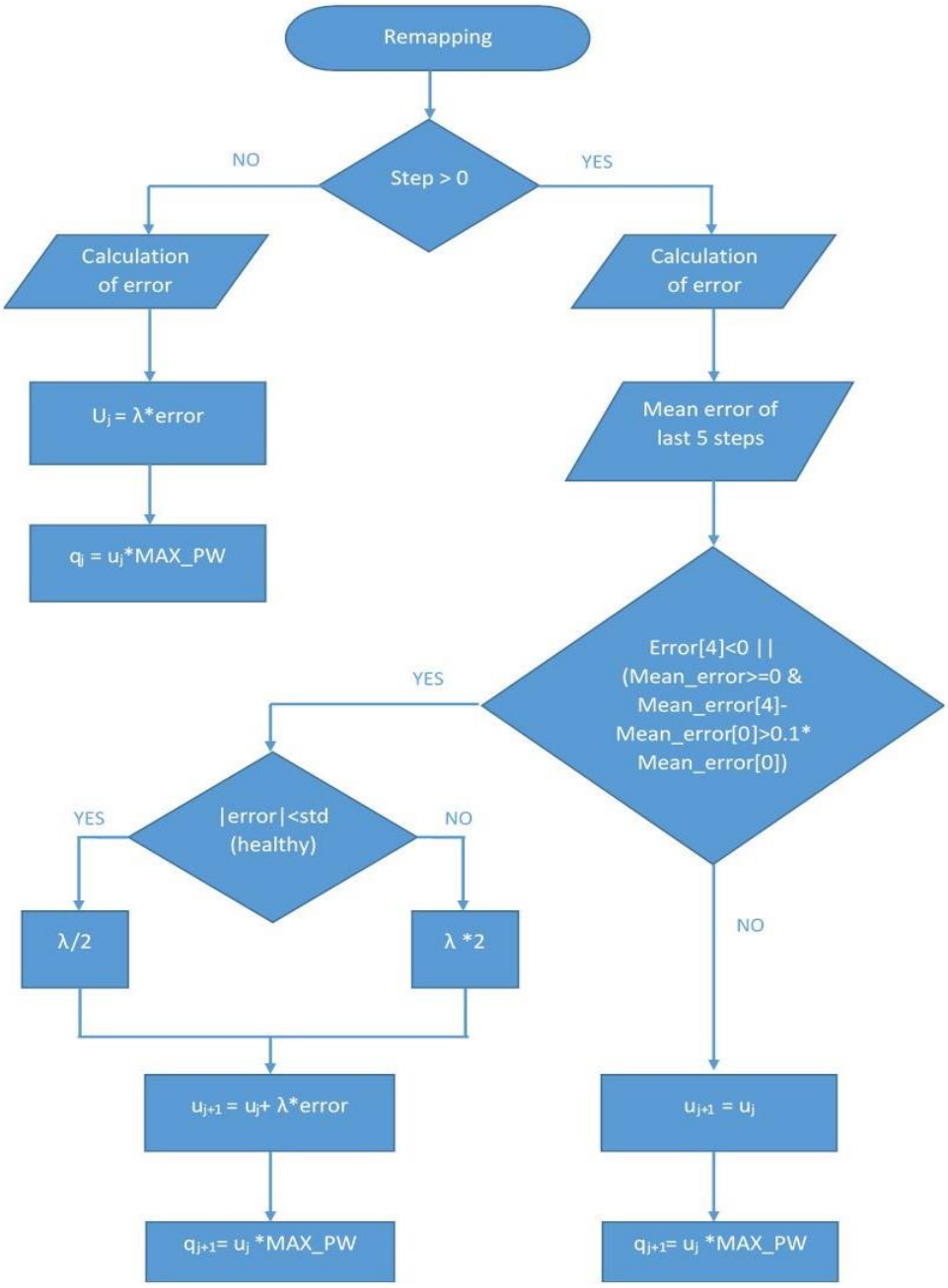

Fig.A In the flow diagram is explained the way in which the ILC works

The error was used to calculate the control variable of the controller, which, multiplied for the maximum value of the chosen pulse width, produces the stimulation profile to be applied to the muscles during the gait phases analyzed. The muscle that was stimulated to promote knee flexion was the gastrocnemius, whereas the tibialis anterior was used to correct the dorsiflexion of the ankle, that could be affected by the pathology and the artificial stimulation of the gastrocnemius. To improve the efficiency of the algorithm, the values of the control variable *u* were modulated in order to obtained an appropriate distribution of stimulation in different conditions.

The algorithm robustness was tested on 7 healthy subjects performing 3 different tasks: normal walking, sudden changes in velocities and walking without knee and ankle flexion.

The results obtained showed that the algorithm was capable to adapt to all tasks requested. In the case of normal walking or sudden velocity changes, low levels of stimulation were given to the gastrocnemius and the tibialis anterior. On the other hand, during walking without knee flexion, the level of stimulation increased and tried to correct both knee flexion and ankle dorsiflexion, in order to reach the reference trajectory.

Through a one way Anova statistical analysis the mean value and the standard deviation of the stimulation profile *q,* for both gastrocnemius and tibialis anterior, were calculated during each task. From the comparison between these parameters, it could be inferred that the mean value of the stimulation profile calculated during walking with a reduced knee flexion was statistically different from the profiles calculated during the other tasks, with a p-value equal to 0.015 for the gastrocnemius and 0.0019 for the tibialis anterior.

In figure B are shown the results obtained from the Anova test.

a)

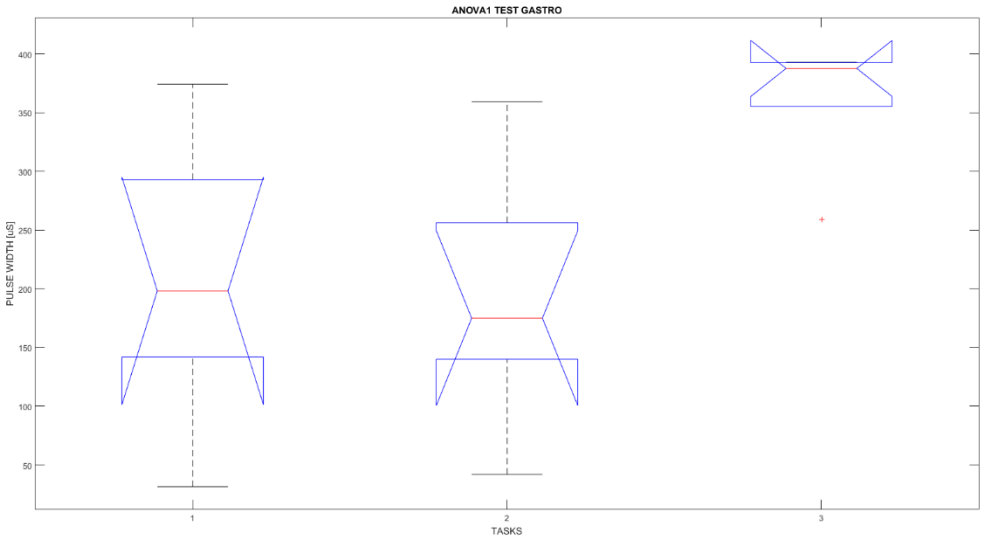

b)

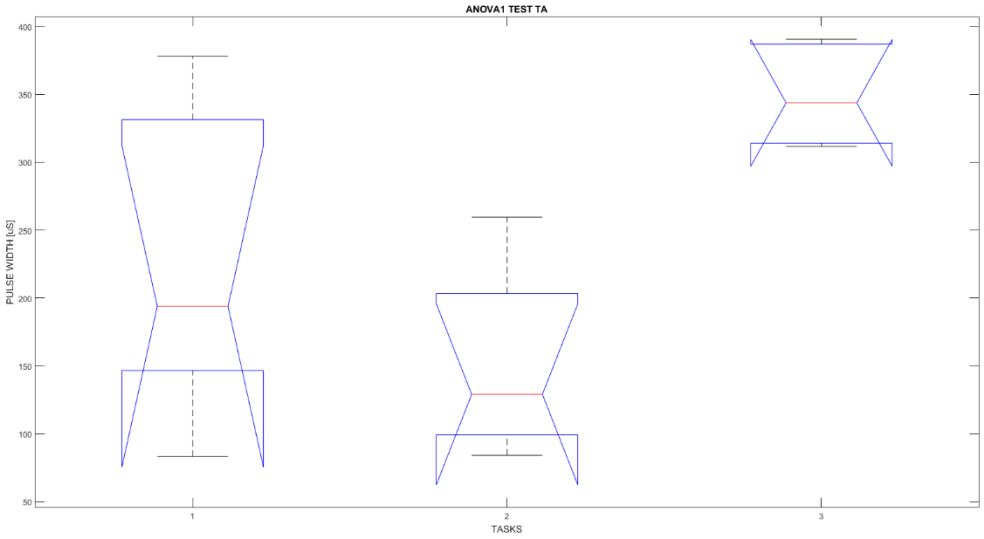

Fig.B. Panel a: a boxplot for each trial regarding the gastrocnemius stimulation is shown, task one corresponds to a normal walking, task 2 correspond to the change in velocity during walking and task 3 refers to walking with a reduced knee flexion. In panel b are shown the same data, calculated for the tibialis anterior.

These results proved that the neuroprosthesis was able to work during different condition of walking, adapting to sudden changes in the walking pattern, and providing stimulation when the subject's current kinematics needed it. However, these very positive results must be completed with a validation recruiting subjects affected by the target pathology. Thus, future developments should perform feasibility studies on SCI subjects, in order to fully test the neuroprosthesis as an assistive, and eventually rehabilitative, aid for SCI subjects.

Sommario

Il termine Spinal Cord Injury (SCI) si riferisce a danni al midollo spinale risultanti da traumi (es. incidenti stradali), da malattie o da degenerazioni (es. cancro) ed è definito come *un danno al midollo spinale che provoca un cambiamento, temporaneo o permanente, nel normale funzionamento motorio, sensoriale o anatomico del midollo* [1].

I soggetti SCI incompleti possono beneficiare della riabilitazione neuro-motoria che sta avendo un notevole sviluppo negli ultimi decenni. Uno dei trattamenti riabilitativi più importanti utilizzati per la riabilitazione a seguito di danni neurologici è la Functional Electrical Stimulation (FES), la quale, come proposto in diversi studi, è in grado di generare contrazioni di muscoli, permettendo dunque lo svolgimento di attività quali la pedalata, il mantenimento della posizione eretta e il cammino. La FES ha effetti sui circuiti del sistema nervoso centrale. Nell'attraversamento del midollo spinale e nella salita verso il cervello, lo stimolo elettrico aumenta l'attività dei circuiti spinali e corticali coinvolti nel movimento. Questo fatto può portare a neuroplasticità sia breve che a lungo termine [2].

L'obiettivo principale del lavoro è stato lo sviluppo di una neuroprotesi, basata su dati acquisiti tramite sensori inerziali e magnetici, per soggetti affetti da SCI, al fine di controllare la flessione del ginocchio e la dorsi-flessione della caviglia durante la preparazione e l'inizio della fase di swing.

Lo sviluppo della neuroprotesi è stato suddiviso in tre blocchi principali: rilevamento in tempo reale degli eventi del cammino, analisi cinematica e Iterative Learning Controller (ILC).

Nel primo blocco è avvenuta l'ottimizzazione di un algoritmo, esistente e validato, attraverso il quale il cammino è stato segmentato utilizzando delle soglie calcolate automaticamente durante la calibrazione effettuata durante i primi 4 passi del soggetto ed aggiornate passo per passo [3]. Questi processi sono stati ottimizzati separando la fase di calibrazione da quello di rilevamento in tempo reale degli eventi e di aggiornamento passo per passo, permettendo così di avere una sola calibrazione all'inizio della prova. L'algoritmo ottimizzato è stato validato, analizzando le metriche di precisone (P), Sensitività (R) e F1-score, calcolata come la media armonica tra le altre due metriche [3], su dati acquisiti durante cinque prove

sperimentali, compiute da due soggetti sani, ai quale è stato chiesto di eseguire cinque diversi protocolli (cammino rettilineo, cambi in velocitò, cambi in pendenza, cambi di direzione, start e stop). I risultati ottenuti hanno mostrato che le P, R e F1-score hanno assunto valori elevati durante tutti i tipi di protocollo proposti, specialmente durante le prove di cammino rettilineo, in cui nessun Falso Positivo (FP) o falso negativo (FN) è stato rilevato durante il rilevamento degli eventi del cammino. In tale protocollo le metriche hanno dunque assunto il massimo valore di 1.

Attraverso questi cambiamenti è stato possibile rilevare gli eventi del cammino dal primo passo e quindi la neuroprotesi è stata in grado di funzionare dall'inizio della prova.

Il secondo blocco è riferito all'analisi cinematica, tramite la quale è stato possibile estrarre le variazioni di angoli al ginocchio e alla caviglia durante il cammino. Sono stati implementati tre differenti algoritmi per raggiungere tale obiettivo: il primo prevedeva l'utilizzo di matrici di rotazione estratte dai sensori inerziali e magnetici, il secondo l'integrazione di dati acquisiti da accelerometri e giroscopi e il terzo l'estrazione degli angoli solo tramite giroscopi, rimuovendo l'eventuale drift creatosi. Gli algoritmi sono stati validati su 12 soggetti sani, durante cammino rettilineo a velocità normale. La terza versione del software, basata sul "detrend" dei giroscopi ha fornito i risultati migliori e per questo motivo è stata scelta per l'estrazione di angoli al ginocchio e alla caviglia nell'applicazione finale.

L'ultimo blocco implementato è stato quello relativo al controllore, di tipo ILC. L'algoritmo ha provveduto all'estrazione dell'errore creatosi tra una traiettoria di riferimento, stabilita a priori, e la traiettoria calcolata, attraverso l'analisi cinematica, durante la preparazione e l'inizio della fase di swing, sia per gli angoli al ginocchio che per quelli alla caviglia.

In figura A è raffigurato il diagramma di flusso che spiega il funzionamento del controllore.

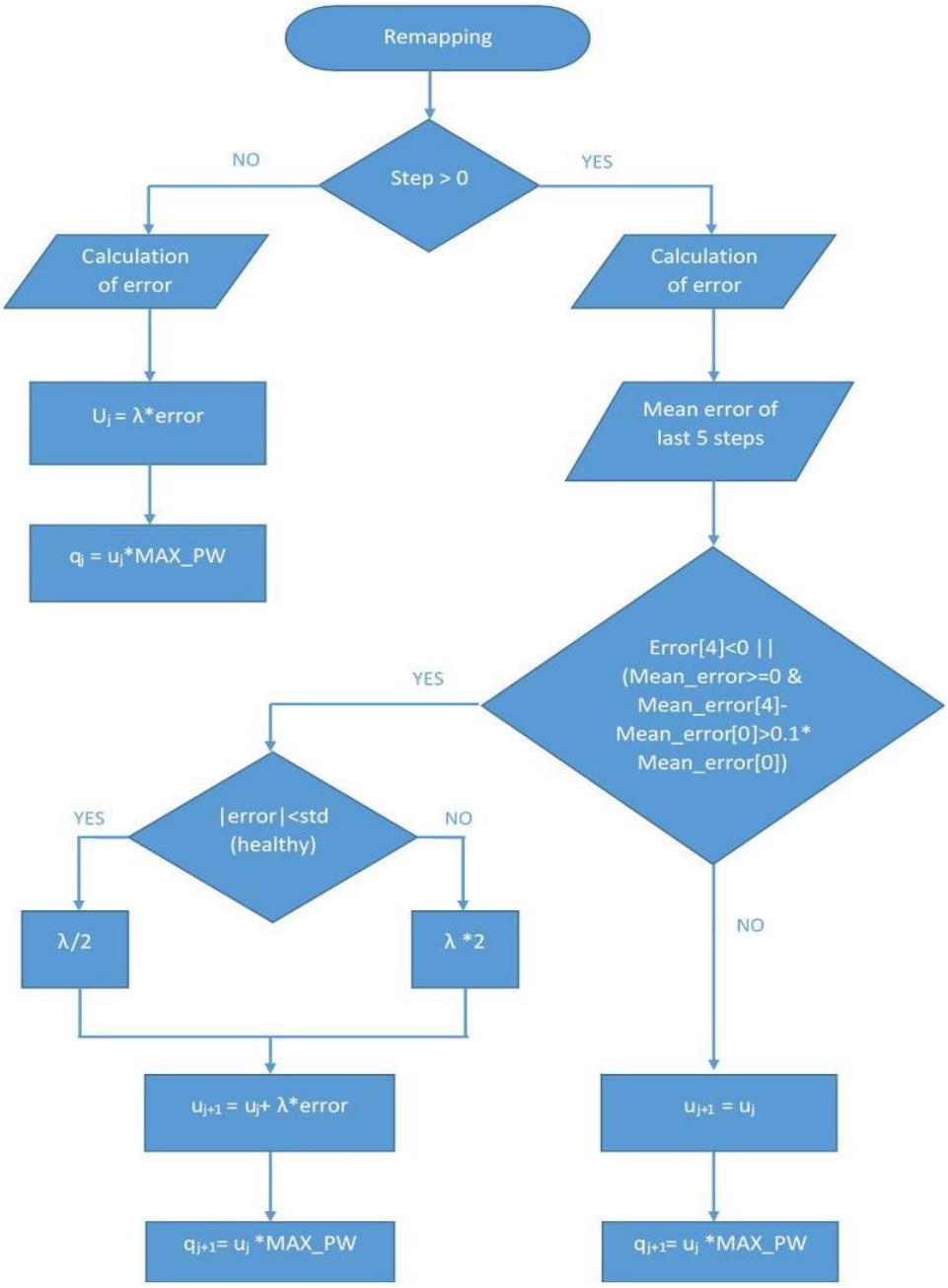

Fig.A Il diagramma a blocchi mostra il funzionamento del controllore

L'errore è stato successivamente usato per calcolare la variabile di controllo del controllore, la quale, moltiplicata per il massimo valore di pulse width scelto, ha prodotto il profilo di stimolazione da applicare ai muscoli. Il muscolo stimolato per promuovere la flessione di ginocchio è stato il gastrocnemio, mentre il tibiale anteriore è stato stimolato al fine di correggere la dorsi-flessione della caviglia, che potrebbe essere alterata sia dalla patologia sia dalla stimolazione artificiale del gastrocnemio. Al fine di migliorare l'efficienza dell'algoritmo i valori della variabile di controllo *u* sono stati modulati in modo da ottenere risposte in termine di distribuzione della stimolazione appropriate in diverse condizioni.

La robustezza dell'algoritmo è stata testata su 7 soggetti sani ai quali è stato richiesto di svolgere tre differenti prove: cammino normale, cambi improvvisi di velocità e cammino senza flessione di ginocchio e caviglia. I risultati ottenuti mostrano che l'algoritmo è stato in grado di adattarsi a tutte le prove effettuate. In caso di cammino normale o cambi improvvisi di velocità, sono stati forniti al gastrocnemio e al tibiale anteriori bassi livelli di stimolazione. Al contrario, durante il cammino senza flessione di ginocchio e caviglia, vi è stato un incremento dei livelli di stimolazione forniti ai muscoli al fine di correggere sia la flessione del ginocchio che la dorsi-flessione della caviglia, in modo da avvicinarsi alla traiettoria di riferimento.

Attraverso un'analisi statistica basata su un test Anova ad una via, il valore medio e la deviazione standard del profilo di stimolazione *q,* sono stati calcolati durante le diverse prove. Attraverso il confronto dei parametri estratti durante le tre prove, si è potuto dedurre che il valore medio del profilo di stimolazione, calcolato durante cammino con scarsa flessibilità di ginocchio è statisticamente differente dai valori medi del profilo di stimolazione calcolati durante le altre due prove, con dei valori di p-value pari a 0.015 per il gastrocnemio e 0.0019 per il tibiale anteriore.

In figura B sono mostrati i dati estratti dal test Anova.

a)

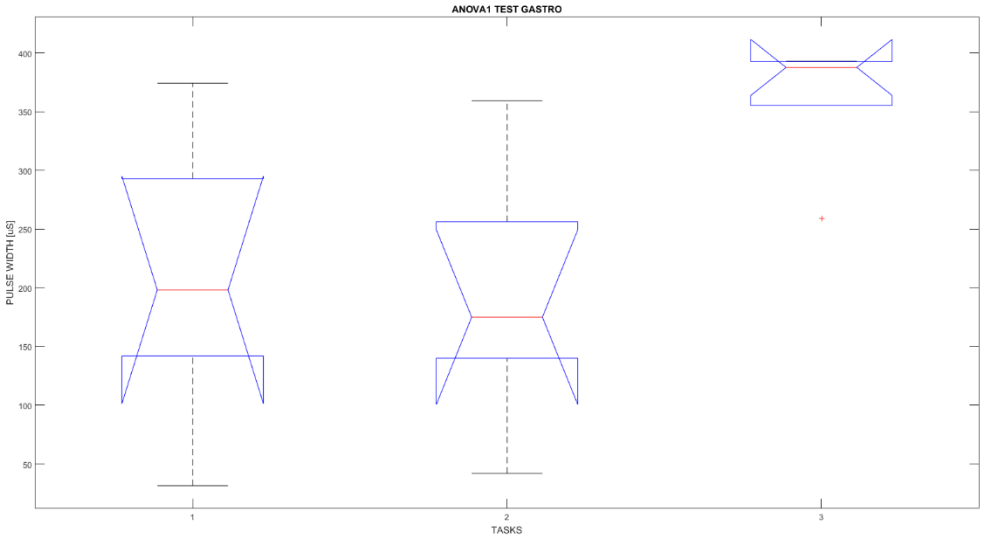

b)

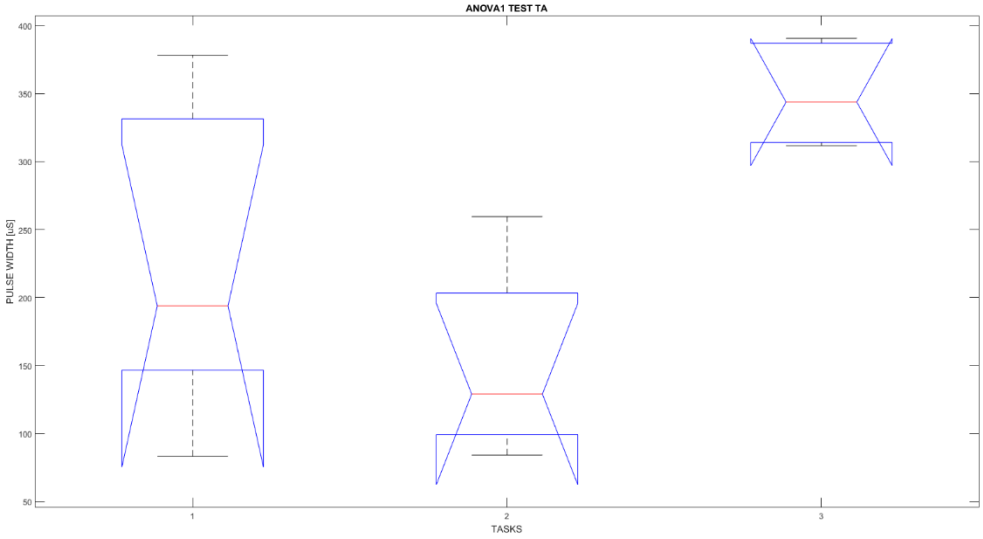

Fig.B. Pannello a: il valore medio dei profili di stimolazione forniti al gastrocnemio è raffigurato per tutte e tre le prove effettuate, con la sua deviazione standard. Nel pannello b sono riportati gli stessi dati riferiti al tibiale anteriore.

Questi risultati dimostrano che la neuroprotesi è stata capace di funzionare sotto diverse condizioni di cammino, adattandosi a cambi improvvisi nello schema del cammino e fornendo stimolazione artificiale quando la cinematica dei soggetti lo richiedeva.

Tuttavia questi risultati molto positivi necessitano di essere completati tramite una validazione su soggetti affetti da una patologia. Quindi, gli sviluppi futuri del lavoro prevedono il compimento di studi di fattibilità su soggetti affetti da SCI, al fine di testare in modo completo la neuroprotesi, come un dispositivo assistivo, ed eventualmente riabilitativo, per soggetti affetti da SCI.

1. Introduction and State of Art

1.1. Spinal Cord Injury

The term Spinal Cord Injury refers to damage to the spinal cord resulting from trauma (e.g. a car crash) or from disease or degeneration (e.g. cancer) and it is defined as *an insult to the spinal cord resulting in a change, either temporary or permanent, in the cord's normal motor, sensory, or autonomic function*. Patients with spinal cord injury usually have permanent and often devastating neurologic deficits and disability [1].

It is very important to make a distinction between the different types of damages in order to choose the appropriate rehabilitation treatment for the subjects.

For this aim, the American Spinal Injury Association (ASIA), published an internal classification that is still widely used to document sensory and motor impairments following SCI. It is based on neurological responses, touch and pinprick sensations tested in each dermatome, and strength of the muscles that control ten key motions on both sides of the body, including hip flexion (L2), shoulder shrug (C4), elbow flexion (C5), wrist extension (C6), and elbow extension (C7). Traumatic spinal cord injury is classified into five categories on the ASIA Impairment Scale [1].

- **A** indicates a "complete" spinal cord injury where no motor or sensory function is preserved in the sacral segments S4-S5.
- **B** indicates an "incomplete" spinal cord injury where sensory but not motor function is preserved below the neurological level and includes the sacral segments S4-S5. This is typically a transient phase and if the person recovers any motor function below the neurological level, that person essentially becomes a motor incomplete, i.e. ASIA C or D.
- **C** indicates an "incomplete" spinal cord injury where motor function is preserved below the neurological level, and more than half of key muscles below the single neurological

level of injury have a muscle grade less than 3 (i.e. M0: no contraction, no muscle movement, M1: trace of contraction, but no movement, or M2: movement with gravity eliminated).

- **D** indicates an "incomplete" spinal cord injury where motor function is preserved below the neurological level and at least half of the key muscles below the neurological level have a muscle grade of 3 or more (I.e. M3, M4 or M5: muscle can movement against gravity (M3) or with additional resistance (M4 and M5)).
- **E** : If motor and sensation function in all segments are all graded normal and the patient had neurological deficits from SCI before, than the grade is E.

Based on this definitions proposed by ASIA, it is possible to define complete SCI as an absence of sensory and motor functions in the lowest sacral segments, and incomplete SCI as a preservation of sensory or motor function below the level of injury, including the lowest sacral segments

Incomplete spinal-cord injured subjects can benefit from neuro-motor rehabilitation, which has gained popularity in the last decades. The main goals of rehabilitation are prevention of secondary complications, maximization of physical functioning and reintegration into the community [4]. It is in this scope that the present work has been developed, as a neuroprosthesis to support incomplete SCI subjects during gait.

In the last decades one of the most important rehabilitative treatment used to recover from damages induced by neurological damages is Functional Electrical Stimulation, that, as purposed by E J Nightingale et.al, it is able to generate purposeful contractions of paralyzed muscles, thereby enabling functional activities such as cycling, standing and stepping. In addition to increasing functional upright mobility, chronic use of FES may offer therapeutic benefits such as decreasing muscle spasm, increasing blood flow to stimulated areas, increasing muscle strength in paralyzed muscles and improving cardiorespiratory fitness [5].

In section 1.2 it will be presented FES in its general principles and in section 1.2.1 its applications in rehabilitation for SCI subjects.

1.2. Functional Electrical Stimulation

Functional electrical stimulation (FES) is a technique that uses electrical stimulation to fully or partially recover compromised motor activity. It is used to activate muscles affected by paralysis or paresis in order to obtain a functional movement.

The main condition to use this technique is that the peripheral nervous circuits and the last neuron have to be intact to provide the transmission of electrical pulse to the muscle.

The nerve cells and muscle cells are excitable, inside them there is the generation and the propagation of the action potential. Usually muscular cells have a bigger activation threshold than nervous cells. When a muscle is activated, firstly there is activation of the nervous fibers inside the muscle then there is the muscular activation.

To perform FES, a pair of electrodes acting respectively as anode and cathode are needed, between whom a current flows and generates a depolarization of the nerve or the muscle. Using electrical stimuli above threshold, an action potential could be generated in the axons as shown in figure 1.

The mechanism followed by FES is the following: the stimulator electrode create a local electric field that depolarizes cellular membrane of the nearest neurons. If the depolarization reaches the critical threshold, an action potential is generated and it goes in both ways of the axons, starting from the stimulation site. The action potential that travels in the distal way is transmitted to the neuromuscular junction and generates muscular contraction.

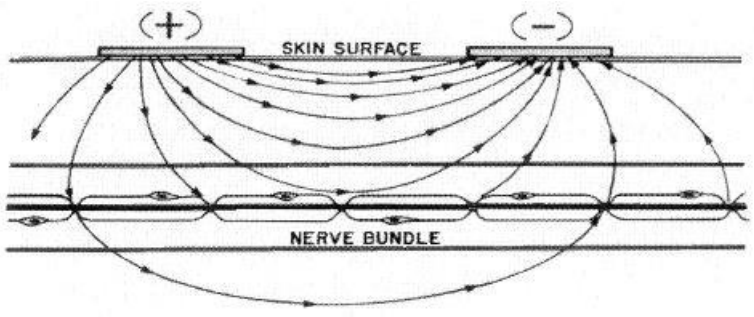

Fig.1. In the image is shown a schematic representation of the electric field inside the tissues. If the amplitude of the field is sufficiently high an action potential starts in the nerve bundle [6].

Using artificial stimulation, the propagation way depends on the site of stimulation and could be opposite to the physiological direction (antidromic way). In case of mixed nerves, compounds by sensory and motor fibers, the stimulation can produce those effects [7]:

- Ortodromic propagation through motor pathway, from the center to the periphery. There is a direct stimulation of the muscular fibers. The result is the M-wave that is the sum of all action potentials generated by the simultaneous excitation of the axons; usually this phenomenon corresponds to the highest mechanical effect.
- Ortodromic propagation through sensory pathway, from periphery to center. These signals can activate different type of reflexes. One reflex can be the “feedback reflex”, it occurs when the amplitude of the stimuli is high, generates a flexor pattern activation, sometimes this reflex is used to activate synergistically a significant number of muscles stimulating only one site.
- Antidromic propagation through motor pathway or through the sensory pathway, from the center to the periphery. If the signal arrives to the periphery through the first pathway, the moto-neuron could be activated, while, if the signal arrives from the sensory pathway, there are no particular effects on receptor terminations.

Since the activation threshold of nervous fibers is lower than that of the muscles, the electrical stimulation actives the motor neurons rather than the muscle. Usually the stimulation pulse is a square wave followed by a wave with opposite sign that is used to nullify the net flow of charge.

It is possible to control the length of the muscle’s contraction by setting some parameters during the application of the stimulus, as shown in figure 2.

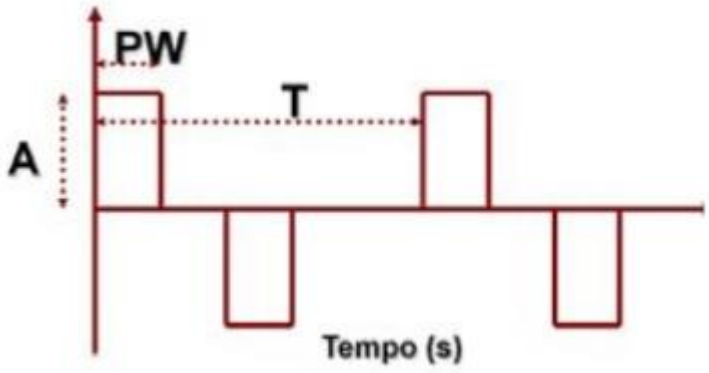

Fig.2. (A) pulse amplitude, (PW) pulse width, (T) period [7].

- Pulse amplitude (A)

Increasing the amplitude of FES pulses generates a stronger depolarizing drive that travels deeper into the tissues, usually the stimulation system is controlled in current, rather than in voltage, because it's safer to the patient. Higher amplitude will also depolarize more sensory axons and send a larger sensory volley to the central nervous system, however the amplitude of this sensory volley is limited by antidromic transmission in motor axons; at high amplitudes, antidromic transmission in motor axons blocks orthodromically transmitted signals, reducing the contribution of the central recruitment. Therefore, contractions evoked at maximal amplitudes, that activate all the motor axons to a given muscle, will be driven by activity through peripheral pathways, to generate contractions with central contribution is required a stimulation that minimize this antidromic block.

- Pulse width (PW)

Is the duration of the positive or negative impulse, changing the duration of the pulses alters the relative recruitment of motor and sensory axons.

Short pulse duration preferentially activate motor axons, while using longer pulse duration will recruit more sensory axons.

- Pulse frequency (1/T)

The frequency at which individual pulses are delivered determines the frequency at which action potentials travel along the axons. For contractions generated through peripheral pathways, pulse frequency influences how force generated through successive M-waves summates and contributes to the smoothness and strength of the evoked contractions. For contraction generates using the peripheral pathways electrical stimulation is delivered at frequency high enough to produce fuse contractions, if the frequency is too high, the muscle will be fatigued rapidly.

- Pulse shape

It is usually biphasic in order to remove charged ions inside the tissues that could be dangerous, the sum of the areas of positive and negative waves should be equal to zero.

During physiological activations, all the motor units are recruited by voluntary descending drive that activates first, small and fatigue resistant motor units, followed by larger, fast-fatigable, motor units. However, induced artificial activations present slightly different characteristics.

The stimulation could be performed using different types of electrodes, such as transcutaneous electrodes, percutaneous electrodes and subcutaneous electrodes.
Transcutaneous electrodes are placed on the skin above the nerves or the muscles that have to be activated. The advantages of these electrodes are the noninvasiveness, the simplicity of the technology, the small impedance on the interface, the low dispersion of current, the flexibility, and the easy application on the skin.
In any case, the continuous placement of the electrodes, to obtain the desired response, requires precision and patience, due to the relatively high inter-subject variability. Furthermore, it can be difficult to reach isolated contractions or try to stimulate deep

muscles. Sometimes the stimulation can cause painful sensations due to activation of cutaneous pain receptors. Other disadvantages of using transcutaneous electrodes are the high energy requirements and a slow walking speed [9].

The percutaneous systems use intramuscular electrodes that pass through the skin and are implanted in the muscles that have to be activated. These electrodes have the stimulation surface in contact or inside the muscle. The percutaneous electrodes can activate deep muscles and provide isolated and repeatable contractions.

The implanted systems are used for long period treatments, in this system, the stimulator is implanted so there is no need to connect the patient to an external stimulator. The stimulator receive the instructions using radio waves [6].

When FES is delivered through the skin, axonal activation depends both on the distance of the electrode from the axon as well as axon diameter, first are activated the fibers with a bigger diameter.

During voluntary contractions the activation of the motor units is asynchronous with respect to each other, allowing for fuse contractions to be achieved at relatively low firing rates. Such low firing rates imply a lower metabolic demand for each motor units.

In contrast, using artificial stimulation, motor units discharge synchronously. Thus, to obtain a contraction of comparable force to the physiological activation, a higher motor unit discharge rate is needed. This is particularly true for people with chronic spinal cord injury, due to an inactivity, paralyzed muscles tend to atrophy and slow motor units (fatigue-resistant units) take on characteristics of fast motor units (non fatigue-resistant).

When electrical stimulation is used, one of the major limitation is the limited spatial recruitment of motor units. When the stimulus is applied over the muscle belly, the contraction is mainly superficial due to the large distance from the stimulating electrodes to the deepest motor units. This results in an inability to recruit all of the motor units in a muscle, even at high stimulus amplitudes. A solution to maximize the spatial recruitment is to increase the pulse amplitude, to depolarize additional muscle fibers located at greater distance from the electrodes. However, another way is to maximize the central recruitment

by stimulating over the nerve trunk or increasing the pulse frequency. In both cases, the muscle is more stressed and the fatigue comes quickly, reducing the capacity of the muscle to contract for long time.

If the stimulation is delivered at the level of the nerve trunk, recruitment of the motor axons is independent in relation to axon diameter and is likely superficial within the nerve trunk [2], as shown in figure 3.

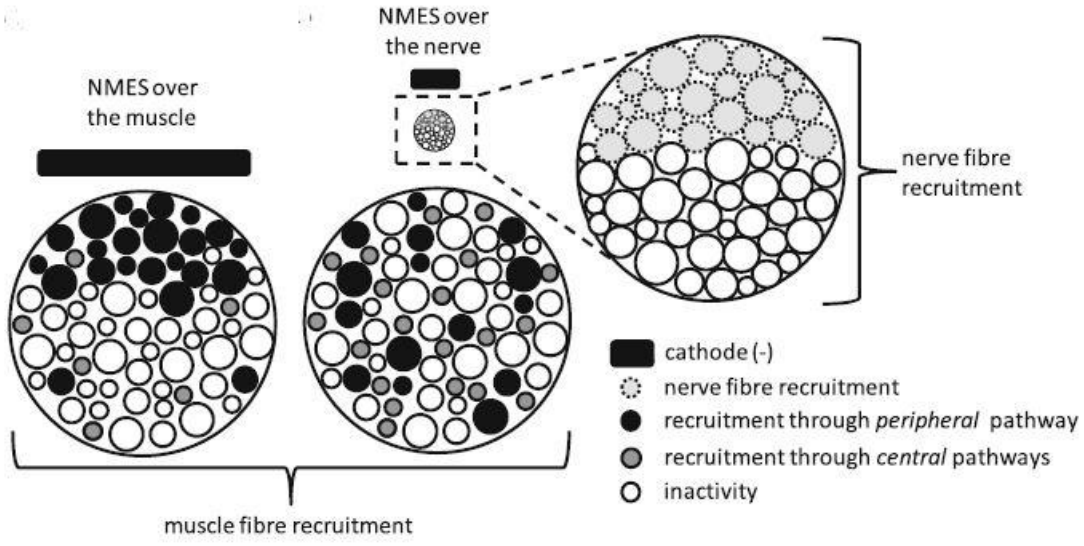

Fig.3. On the left side of the image is shown the muscle fibers recruitment using a stimulation over the muscle, the most superficial fibers are recruited first through peripheral pathways. On the right side is shown the section of a muscle stimulated through a stimulation over the nerve, the recruitment is more homogeneous with a greater spatial distribution, regardless of a superficial recruitment of the nerve fibers [2].

Functional electrical stimulation has some effects on central nervous system circuits. In traversing spinal cord and ascending to the brain, the sensory volley increases activity in spinal and cortical circuits involved in the movement and this can lead to both short-term and long-term neuroplasticity. Generally, after a central nervous system injury and a

prolonged disuse, there is a reduction of the excitability of central nervous system circuits and an impairment of the pathways between the brain and the muscle. During FES there could be an increase of excitability of the central nervous system circuits, the same involved in learning of new motor skills.

1.2.1. FES for rehabilitation of incomplete SCI

Functional Electrical Stimulation plays a very important role in rehabilitation of incomplete SCI subjects, as proposed by E. J. Nightingale et al [5].

In their study the authors use FES to generate purposeful contractions of paralyzed muscles, thereby enabling functional activities such as cycling, standing and stepping. In addition to increasing functional upright mobility, chronic use of FES may offer therapeutic benefits such as decreasing muscle spasm, increasing blood flow to stimulated areas, increasing muscle strength in paralyzed muscles and improving cardiorespiratory fitness [5]. Benefits of FES gait training can be categorized into three main domains: clinical outcomes, such as decrease in muscle spasm and increase in muscle strength (quadriceps), fitness benefits, such as cardiorespiratory fitness and functional gains, such as increase in walking speed and reduction of metabolic cost during gait.

Although previous reviews have investigated these outcomes for interventions such as FES cycling [5], no systematic evaluation has been conducted on the efficacy of FES gait for SCI subjects, because usually FES gait studies include small and heterogeneous population, which leads to statistically under powered results.

1.3. Neuroprosthesis

Neuroprostheses are devices that, through the use FES, interact with the nervous system in order to apply electrical stimuli that can assist impaired patients performing a task. Additionally, through its repeated use, these systems are capable restore some motor, sensory and autonomic functions lost due to spinal cord injury, only by stimulating different parts of the nervous system, as muscles, nerves, spinal cord and brain.

There are some evidences that central nervous system, after a damage, is able to adapt and create new neural pathways to restore voluntary functions. This property of the brain is called *brain plasticity* [2].

Sometimes, under certain conditions, motor neurons, inside the spinal cord, can change synaptic organization in order to re-establish conduction after a lesion. Conduction is established again when electrical stimulation of motor axons matches with the intention of the subject to contract the same muscle that has been stimulated. This process may lead to some restorative changes in the central nervous system.

The use of FES to restore movements in SCI subjects could be tricky because, after a lesion, muscular tissues below the level of injury, are affected by denervation and disuse. Those muscles are no longer able to receive stimuli by the brain and tend to degenerate, losing both volume and strength. Due to this fact, before start using a neuroprosthesis, it is often necessary to train muscles in order to be more fatigue resistant. The training is done by using a surface electrodes, a few days per week, for several months and it leads muscles to generate contractions for a longer period of time, avoiding fatigue.

For patients with neurological deficits, the lower-limb neuroprostheses have mainly been implemented in order to promote standing and walking. These systems can often be divided into external or implanted systems.

An example of commercial, external FES system for SCI subjects is the Sigmedic Parastep that, as shown in figure 4, is a device that uses surface electrodes over quadriceps and gluteal muscles in order to permit knee and hip extension. There are also electrodes over peroneal nerves, to trigger flexor withdrawal reflex [5].

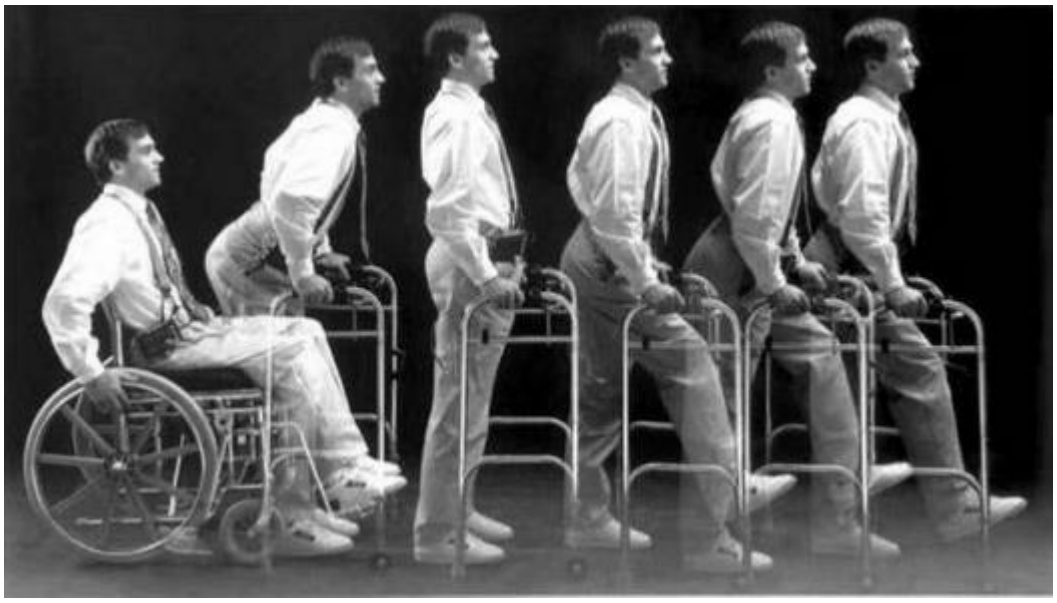

Fig.4. Sigmedic Parastep, this system allows the subject to rise from seated to standing position and also walking for a short distances [9] .

The system enables standing and walking through the use of a preset pattern of stimulation, driven by switch modules, mounted on an instrumented walker [7].

In another study proposed by Thrasher et al., [10], the external system consisted in a stimulator that generates biphasic asymmetrical pulses, through eight electrodes. A constant stimulation was delivered with a constant frequency of 35Hz. The pulse width was modulated between 0 and 300μs and pulse amplitudes changed between 18 and 110mA. A FES program was established to stimulate the whole gait cycle through an open-loop controller. The stimulation sequence was defined, for 4 different muscles, as shown in figure 5.

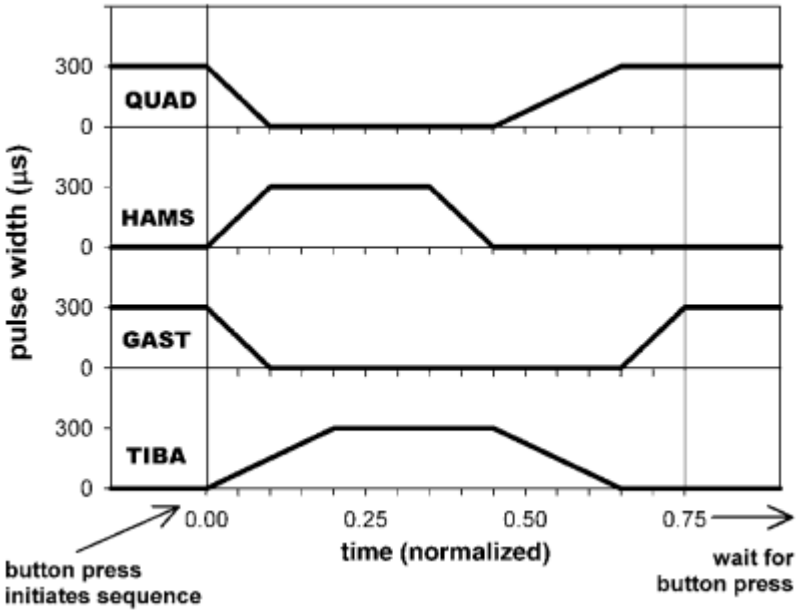

Fig.5. Shape of stimulation for quadriceps, hamstring, gastrocnemius and tibialis anterior during an entire gait cycle [10].

The last example of external system is the one proposed by Sheffler et al.

They implemented a hybrid system, that combined several components, designed for support or stimulation. These type of systems, made from several modules with different and very specific functions, are reliable and quite simple to implement in clinics, with orthotic and prosthetic fabricating capacity [11].One of the main advantages of hybrid systems is that during standing, the support elements can lock the knee joint, allowing the electrical stimulation to be interrupted and reducing fatigue. Another advantage of hybrid systems is that orthosis can protect patients from possible damages resulting from loads applied on them during stance and walking. This is particularly interesting for SCI patients, since they often suffer from osteoporosis [11].

There are other type of systems that can be used as an alternative to external systems, such as implanted systems. An representative example of the latter is the CWRU/VA neuroprosthesis, that used electrical stimulation to activate muscles of trunk, hip, knee and

ankle [12]. This system allowed the wearer to rise from the seated position, maintain standing position and walk for short distances, with the help of a rolling walker.

The configuration of this neuroprosthesis is shown in the figure 6. It consists of an implanted pulse generator, in-line connectors and epimysial implanted intramuscular electrodes. External components are a rechargeable and wearable control unit, with a command ring and transmitting coil, and a clinical programming station.

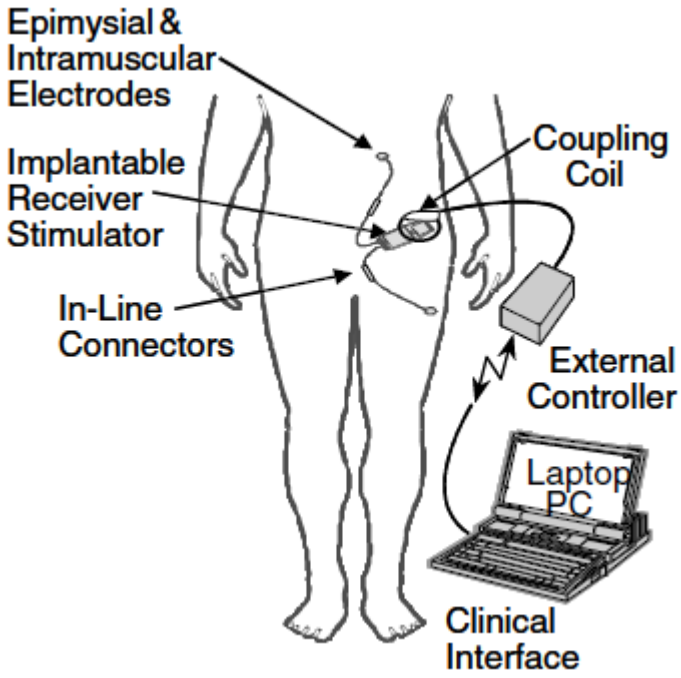

Fig.6. Schematic representation of the CWRU/VA neuroprosthesis [12].

To obtain the standing position, the system stimulated the hip, knee and trunk muscles, while the foot-ankle orthosis preserved and stabilized the ankle. In order to walk for short distances, the system usually targeted hip flexors and ankle plantar flexor or dorsi flexor, depending on the walking deficits of the patient.

The patient controlled the neuroprosthesis using three command buttons, that allowed them to activate or stop a set of pre-programmed stimulation patterns, customized for each subject.

A second example of implanted neuroprosthesis, proposed by the researchers of the university of Utah, consisted of a intrafascicular microelectrode stimulation (IEMS) [8]. This system works with microelectrode arrays, that are placed inside the nerve fascicles. The position of microelectrode arrays allows a physiological recruitment strategy, that generate fatigue resistant and different levels of forces in the hip, knee and ankle muscles. Fatigue resistant is obtained by stimulating moto neurons, which activate, independently, motor unit pools in a specific muscle. Because of intrafascicularly implantation and different length of electrodes, the whole nerve is uniformly populated, that means an access to a small group of axons in the peripheral nerves.

There are evidences that the spinal cord is an integral component in the whole control and regulation system of movement. There are central pattern generators (CPGs), capable to produce rhythmic activity of the legs, without requiring sensory feedback or also integrating sensory feedback and supraspinal signals, in order to generate robust limb movement. It has been demonstrate that CPGs still remain active after spinal cord injuries [8]. There are two neuroprosthesis that directly target spinal cord: epidural cord stimulation and intraspinal micorstimulation (ISMS).

A study on epidural spinal cord stimulation demonstrated that stimulation over lumbar segments of the spinal cord led to rhythmic alternating movements of the legs [13] while intraspinal microstimulation is a system composed by hair-like microwires, implanted in the spinal cord, below the level of the injury. Small electrical pulses are passed through those wires in order to obtain functional leg movements.

The use of this technique has several advantages:

- The microwires are implanted far away from the target muscle, which decreases the possibilities of electrode damages or dislodgment, due to movement of the tissue

- The spinal cord is surrounded by the spinal column, over which are positioned all the implanted electronics
- The lumbosacral enlargement (where wires are placed) is small

In the figure 7 is shown a schematic representation of the location of ISMS system [8].

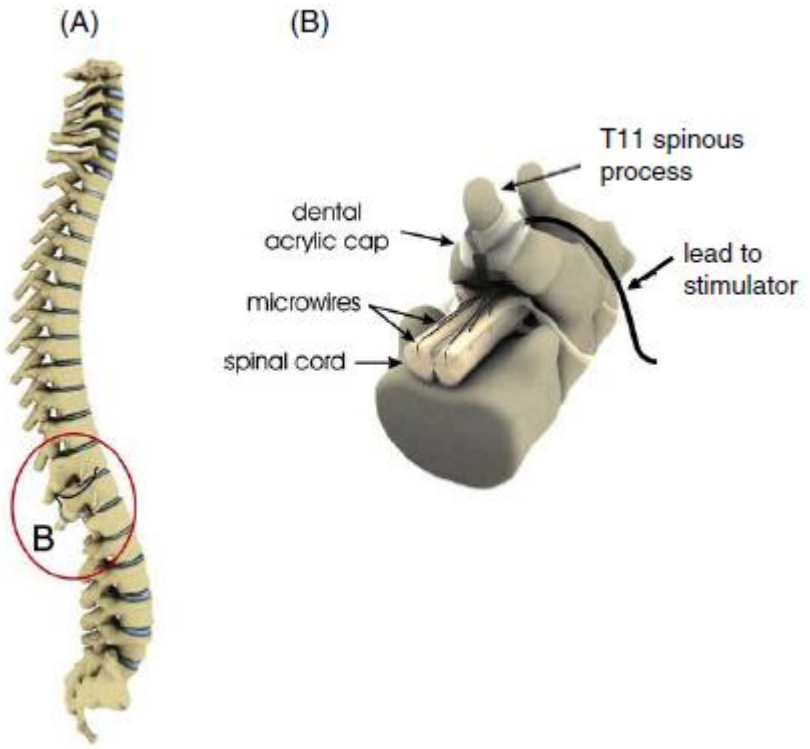

Fig.7. Schematic representation of ISMS implanted system. On the left side is shown the position of the implant on the spinal column, on the right side there is a detailed representation of the implant, the system is anchored to the T11 spinous process [8].

1.3.1. Strategy of control

The control strategy of the neuroprostheses is crucial for its usability and adaptability to the patient's needs. Different solutions have been proposed in the literature, which can be divided into different categories [14] [15]:

- Modelling approach

This approaches models the musculo-skeletal system and the environment, creating a series of equations that have to be solved during the use of the neuroprosthesis. This process implicates that it is necessary to deal with the equations in real time, using restricted set of parameters, which have to be easy to be find on a specific subject. Therefore, a simple but non-linear and physiologically-based model are most commonly used for real-time controller applications. In the case of lower-limb neuroprosthesis for SCI subjects, the input of such model could be the pulse width, whereas the output could be knee joint angle [13]. In this study, variations of knee angle are made by the movement of the shank compared to the thigh, which cannot change its horizontal position during the whole trial. Only knee extensor muscles are stimulated and the movements are performed in the sagittal plane.

The model implemented consists of three blocks: muscle activation, muscle contraction and segmental dynamics, as shown in figure 8.

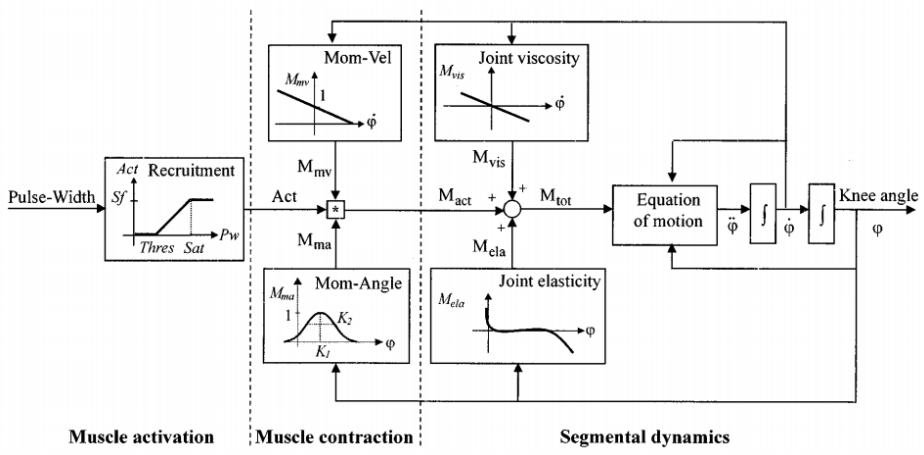

Fig.8. Schematic representation of the model [15].

In the first block, there is the actual muscle activation (*Act*) that is calculated from the stimulation pulse width. The activation dynamic is modeled using a linear recruiting function, characterized by a threshold pulse width, a saturation pulse width and a scaling factor.

Inputs of muscle contraction block are angle and velocity of the knee, the output of the second block is the active muscle moment.

In the third block, total moment is obtained and in a second step the inverse muscle contraction is modeled.

- Open-loop

The characteristic of the open-loop controller is that uses fixed stimulation trains to reach the desired output, even if the movement performed was not expected. The stimulation is triggered by manual or heel switches or measures extracted from the task. To use this type of controller all the stimulation parameters have to be defined in order to obtain the desired task or movement. Some restrictions occurs using this type of control system, in fact, there is no compensation of external disturbances, it is not adaptable to the fatigue of muscles involved in the stimulation and the movement is fixed and is equal for all the period of the trial [14].

Figure 9 shows a schematic representation of a possible open-loop control system.

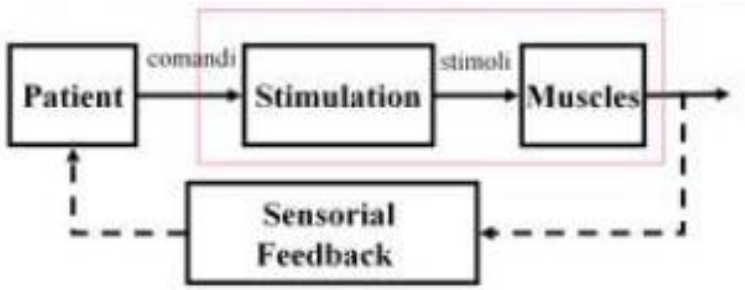

Fig.9. Schematic representation of the open loop controller [15]

Referring to the study proposed by Ferrain et al, [13] it was possible to estimate the pulse width necessary to perform a desired trajectory for knee angle. This type of controller is often preferred at clinical site because of its simplicity. On the other hand, it needs an initial and periodical adjustment in stimulation patterns, for individual patients. Open loop controllers cannot eliminate disturbances as muscle fatigue and external load [12-15].

- Feedback control

Proportional Integrative Derivative (PID) is an example of feedback control, which continuously calculates an error value as the difference between desired and obtained signal. The main goal of the PID controllers is the correction of the error calculated. In order to reach this goal three aspects of the error are taken into account. It is proportional to the current error (P), it is integrative with respect to error history (I) and the derivative part (D) it is referred to the changes of the error over time.

The advantages of using a PID controller are that the stimulation changes according to the error and the controller can handle and compensate unforeseen events. There are also negative aspects using this type of control system, in fact, to set the three parameters (P,I,

D), experimental procedures, that result quite complex for biological system like human being, are needed. In figure 10 is shown a schematic of a PID controller.

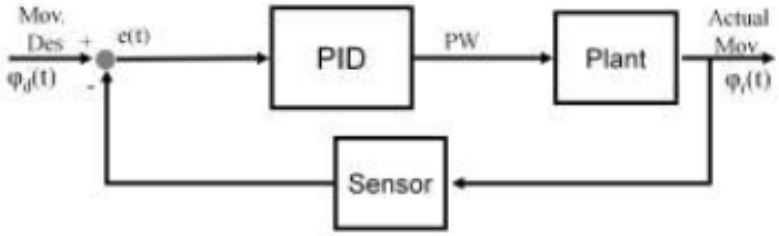

Fig.10. Schematic representation of the PID controller [15]

- Feedforward and Feedback control

It is a combination of an open loop and a feedback controller in which, the feedback controller, is used to compensate model errors and disturbances. The idea is to use a feed-forward model that remap the main characteristics of the system that has to be controlled and a PID controller only for the feed-back loop. The use of this control system provide a reduction of the controller delay due to the presence of the feedforward inverse model.

Some limits of these systems are that the inversion of the model could be complex, the modelization is done with fixed parameters, but the system taken into account, is time variant and the personalization of the algorithm for each subject it's quite difficult to implement. In figure 11 there is a representation of the model.

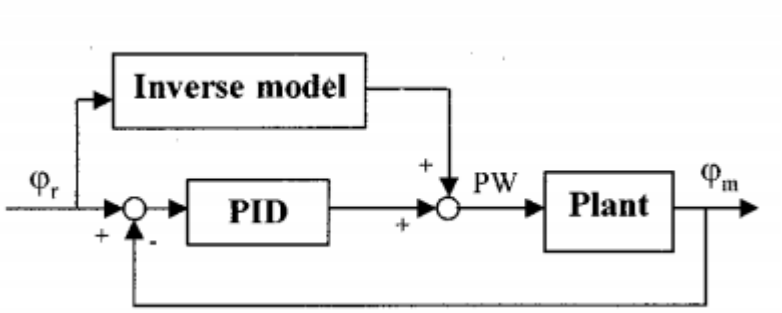

Fig.11. Combination of feedback and feedforward controller [13].

- Adaptive control

These systems allow to follow and control the output, taking into account that external system parameters can change during time. In this control systems, the inverse dynamic model give the predicted input, both to the plant and the direct dynamic model, as shown in figure 12.

The error, calculated between knee angle, predicted by the direct dynamic model, and the one resulting from the plant, controls the adaptation mechanism that changes parameters inside the inverse and direct model.

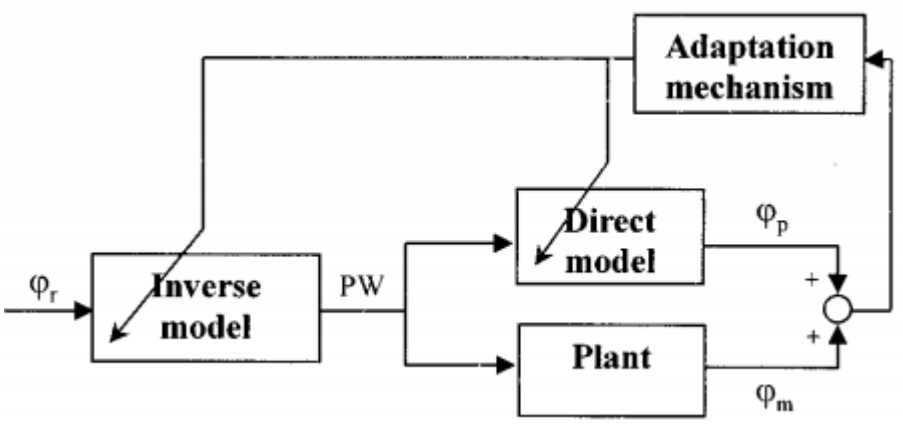

Fig.12. Adaptation controller [15]

1.4. Main goal

The main goal of the work is the development of a closed-loop FES gait neuroprosthesis for spinal cord injured patients. In order to reach this goal, the implementation of the neuroprosthesis was divided into three main parts. The first part concerned the extraction of gait events through the Real-Time Detection algorithm, the second included the calculation and the analysis of knee and ankle kinematic and the third was about the implementation of an Iterative Learning Controller (ILC). A previous validated version of the RTD algorithm was optimized, in order to find the most important events during gate (Initial Contact, End Contact and Mid Swing), from the first step. The second part consisted in the development of kinematic algorithm in order to extract the variation of knee and ankle angles during gait, based on data acquired from inertial sensors.

The third part was based on the development of a closed-loop controller, Iterative Learning Controller (ILC).

The controller compared data acquired during online trials with a known reference, in order to correct knee and ankle angles during walking. Two intensities of stimulation were calculated from the ILC algorithm: one that led to knee flexion by stimulating the gastrocnemius, the other one that led to ankle dorsiflexion, in order correct plantar flexion induced by stimulating the gastrocnemius. The choice was to develop a controller for the right leg, but it was also possible to control the gait phases analyzed for the left leg and also for both legs simultaneously.

1.5. Organization of the work

The work is divided into 4 chapters. After an introduction in which have been discussed the concept of Spinal Cord Injuries (SCI), Functional Electrical Stimulation (FES) and neuroprosthesis based on FES, in chapter 2 are described the materials and methods used to reach the main goal. The chapter is subdivided into two main sections: the first one regards the hardware used to collect data and stimulate, the second one in which is described the algorithm used to develop the neuroprosthesis. The second section is divided in three paragraphs: the first describes Real-Time detection algorithm, the second describes three versions of kinematic analysis algorithms and the third explains the development of the Iterative Learning Controller.

In chapter 3, are shown the results obtained, for each section of chapter 2.

In chapter 4 the results obtained are discussed, the conclusions are stated and the future development are proposed.

2. Materials and Methods

2.1. Hardware

The hardware used to test the algorithms implemented was based on two different experimental setup. The first, used at the CSIC laboratory in Madrid, was made of 6 Technaid inertial sensors, 3 for each leg, placed on thigh, shank and foot. The IMU sensors contained accelerometers to extract 3D linear accelerations, gyroscopes to extract 3D angular velocities and magnetometers to extract 3D magnetic field. They worked with a sampling frequency of 1 kHz and had a built in calibration to eliminate axes misalignment, sensibility and compensate the measurements due to external temperature changes. In addiction a Kalman filter was implemented in order to estimate absolute 3D orientation [17].

The improvement of the Real-Time Detection algorithm and the three version of the kinematic, that will be described in the next section, were tested with this experimental setup.

The second experimental setup used in Politecnico di Milano, was composed of 5 inertial sensors (MTx, Xsense technologies B.V.), 3 for the right leg, placed on thigh, shank and foot, and 2 for the left leg, placed on shank and foot.

The sensors contained accelerometers, MEMS solid state with a capacitive readout, in order to extract 3D linear accelerations, gyroscopes, MEMS solid state, monolithic with a capacitive readout in order to extract angular velocities and magnetometers, with thin film magneto-resistive, to estimate 3D absolute orientation [18].

The orientation of the sensors was computed by Xsens Kalman Filter for 3 degrees-of-freedom orientation (XKF-3). XKF-3 used signals of the rate gyroscopes, accelerometers and magnetometers to compute a statistical optimal 3D orientation estimate of high accuracy with no drift for both static and dynamic movements.

The design of the XKF-3 algorithm could be explained as a sensor fusion algorithm where the measurement of gravity (by the 3D accelerometers) and Earth magnetic north (by the 3D

magnetometers) compensated for otherwise slowly, but unlimited, increasing (drift) errors from the integration of rate of turn data (angular velocity from the rate gyros). This type of drift compensation is often called attitude and heading referenced and such a system is often called an Attitude and Heading Reference System (AHRS) [18].

XKF-3 stabilizes the inclination (i.e. roll and pitch combined, also known as “attitude”) using the accelerometer signals. An accelerometer measured gravitational acceleration plus acceleration due to the movement of the object with respect to its surroundings. XKF-3 used the assumption that on average the acceleration due to the movement was zero. Using this assumption, the direction of the gravity could be observed and used to stabilize the attitude [18].Those sensors were used to extract references for the Iterative Learning Controller and to test it during experimental trials. The third element used in the experimental setup was the stimulator, to provide FES. Two surface electrodes were used, one placed on the gastrocnemius of the right leg, in order to provide knee flexion and the other one placed on tibialis anterior of the same leg, in order to compensate plantar flexion induced by stimulating gastrocnemius.

2.2. Software

In this section are explained the algorithms on which is based the neuroprosthesis, divided into three main parts: Real-Time Detection, Kinematic Analysis and Iterative Learning Controller.

The first part allows the detection of gait phases, the second to extract knee and ankle angles and the third part refers to the algorithm that control the stimulation given to the muscles.

2.2.1. Real-Time Detection

The Real-Time Detection algorithm is an adaptive algorithm able to identify six different phases of gait cycle in real time [3].

In order to obtain those phases, the algorithm uses two inertial sensors, placed on the shanks of each leg.

The algorithm works as a state machine, where one state corresponds to a gait phase. To detect six gait phases (three per leg), the angular velocity of the shank in the sagittal plane, and the flexion/extension angle of the shank, referred to the vertical axis, are used.

For each leg are detected three events: the first contact of the foot with the pavement (Initial Contact, IC), the last contact of the foot (End Contact, EC), and the point of maximum angular velocity of the leg during swing (Mid Swing, MS), as shown in figure 13.

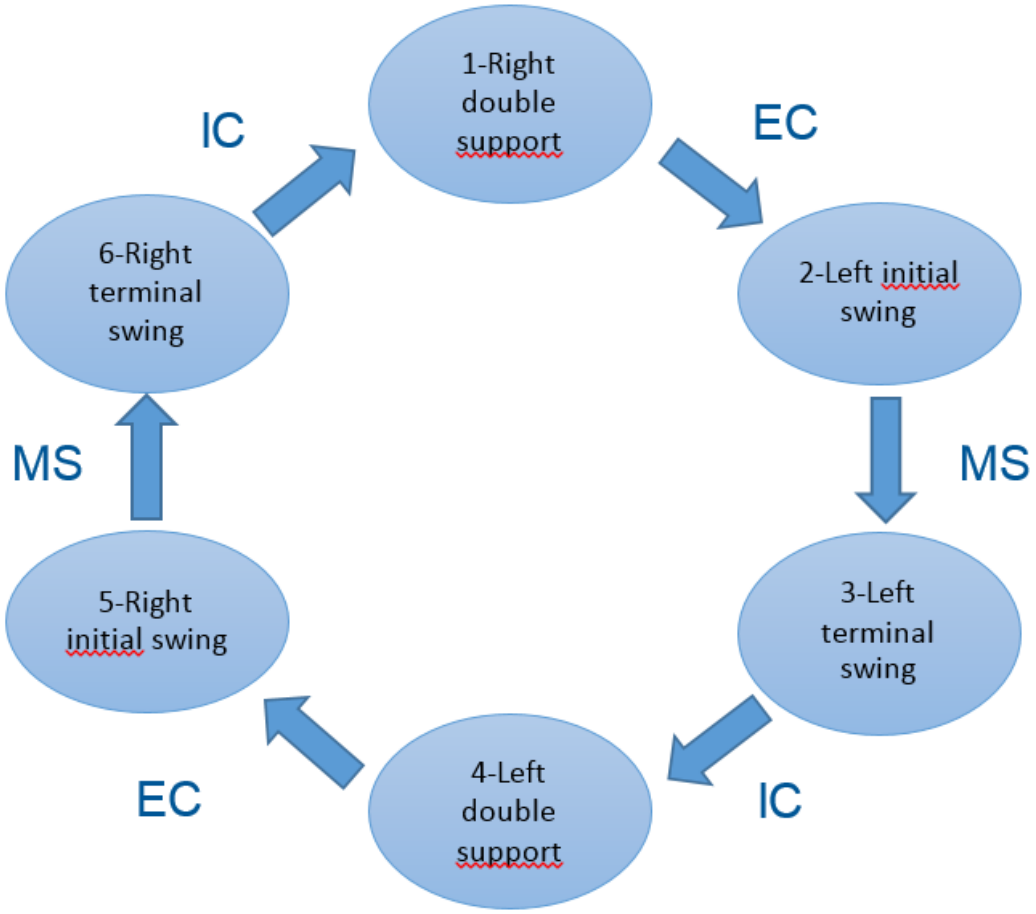

Fig.13. Schematic representation of the State Machine, there are shown the six gait phases and six (three per leg) gait events that control the change of state.

The first threshold (IC) is defined as the minimum of the flexion/extension angle, End Contact is found as the minimum of angular velocity and Mid-Swing is detected as soon as the flexion/extension angle is equal to zero. In figure 14 are shown all the thresholds related to the kinematic of the shank (angular velocity and flexion/extension angle).

The algorithm uses another threshold, called AN, that is defined as the value of the flexion/extension angle that correspond to the End Contact detection. This parameter is used to start to search a new End Contact event.

Based on those events, six different phases during gait cycle can be identified: Left/Right Double Support, Left/Right Initial Swing, and Left/Right Terminal Swing.

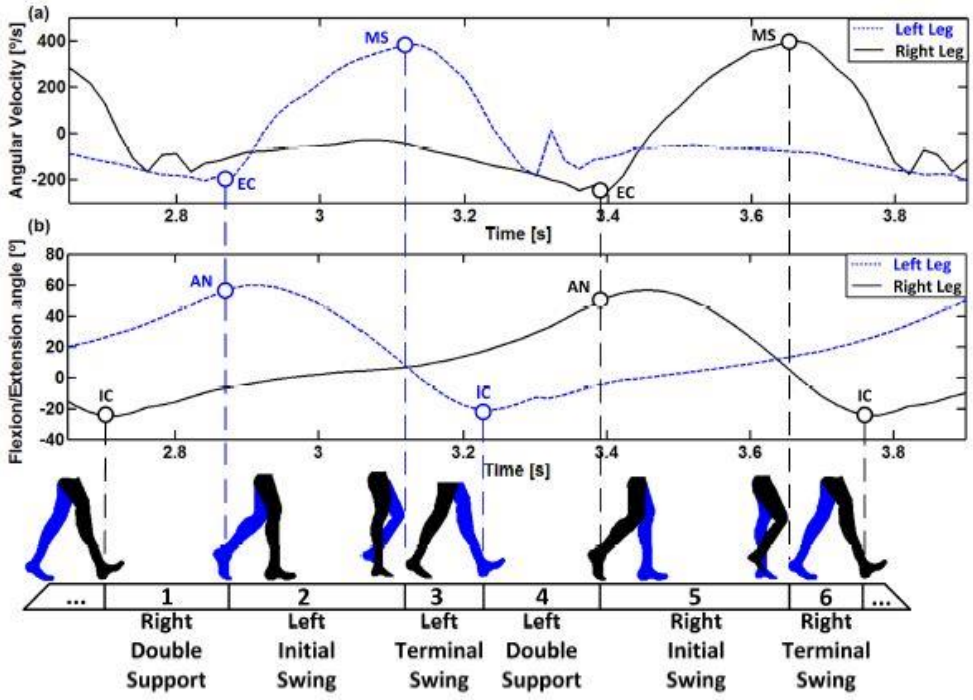

Fig.14. On the top panel is shown angular velocities of the shanks, on the bottom one is represented the flexion/extension angle of the shanks respect to a vertical axis. There are also shown the thresholds that define the six gait phases, (EC) End Contact, (MS) Mid-Swing, (IC) Initial Contact and (AN) that is the value of flexion/extension angle that correspond to the End Contact of the same leg [3].

The RTD algorithm can be divided in three part: Calibration, Real-Time, Update [3].

- Calibration

The calibration is performed automatically analyzing at least the first five steps of the subject. During these five steps all the thresholds are calculated in order to identify the initial values of the algorithm, which are used during the real-time detection, that starts immediately after the calibration. In the new version of the work, the calibration is separated from the real-time detection, the new algorithm saves all the parameters obtained during

the calibration in a txt file, afterwards this file is loaded in the program in order to start immediately the new task without the need of redoing the calibration procedure for each trials.

- Real-Time Detection

The real time detection is based on a state machine, in this part of the algorithm there is a signal processing on the four signal of interest (angular velocity of left and right leg, flexion/extension angle of left and right leg), a first-order low-pass FIR filter with a cutoff frequency of 14 Hz, this filter was selected to optimize the reduction of high frequency noise and the filter delay. Afterwards the algorithm search independently the gait events.

- Update

This part of the algorithm run simultaneously to the real time detection and update the thresholds using the newest correct gait events. At this point there is another processing of the signal, a 10^{th} order low-pass equiripple FIR filter with linear phase and cutoff frequency of 4 Hz, thus filtering provide a gait event detection that is delayed but at the same time more reliable with respect to the real time detection explained in the previous point. The quasi real-time detection is used to correct any errors that could be occurred during the real-time stage.

The improved algorithm was validated on two male healthy subjects, in five different conditions. Each subject repeated each task three times. The experimental setup used to acquire data was based on six Technaid sensors, placed on thigh, shank and foot of each leg.
The tasks performed were the following:

- Straight walk for 20 steps
- Change in velocity: 5 steps at normal speed – 5 steps fast – 5 steps slow – 5 steps at normal speed
- Change in slope: 5 steps straight – 6 steps on a ramp

- Change in direction: 4 steps straight – turn of 45 degrees to the left, 4 steps – 4 steps straight – turn of 45 degrees to the right, 4 steps – 4 steps straight
- Start and stop: 5 steps – stop – 5 steps – stop – 5 steps

Each subject performed a calibration trial in order to save thresholds on a file, that was uploaded at the beginning of each experimental trial.

The validation of the improved algorithm was performed in terms of accuracy, calculated with the metrics, Precision (P), Recall (R) and F-1 score defined as [3] :

$$\mathrm{P} = \frac{\mathrm{TP}}{\mathrm{TP+FP}} \quad (1)$$

$$\mathrm{R} = \frac{\mathrm{TP}}{\mathrm{TP+FN}} \quad (2)$$

$$\mathrm{F1} = 2\frac{\mathrm{P*R}}{\mathrm{P+R}} \quad (3)$$

in which TP correspond to True Positive, FP to False Positive, FN to False Negative and F1-score, defined as the harmonic mean of P and R, was calculated, as shown in eq. 3. These values were found referring to all the gait phases detected, during all the task performed by two healthy subjects, repeated three times.

The results obtained during the validation of the improved algorithm will be shown in section 3.1. The original version of the algorithm was implemented to facilitate separation between calibration and real time detection of events so, likely, results will show a correct detection of gait phases from the first step, whit high values the metrics analyzed to compute the accuracy.

2.2.2. Kinematic analysis

The main aim of the kinematic analysis is the extraction of knee and ankle angles during walk, in different conditions (changes in speed, velocity, slope). In this section are presented three different algorithms implemented in order to reach this goal. Each of those algorithms is based on different techniques to extract angles during walk. The first one is based on rotation matrix, the second on integration of data collected from gyroscopes and accelerometers and the third is based on data collected from gyroscopes corrected in order to remove the existing linear trend.

2.2.2.1. Rotation matrices

The algorithm collected data from accelerometer, gyroscope and magnetometer placed inside Technaid inertial sensors, as explained in section 2.1, and filled a 3x3 matrix with values of direction cosines, referred to Earth's reference system, of each sensor used in the experimental setup.

Three matrices were calculated, one per sensor: one for thigh, one for shank and one for foot.

Rotation matrices that refers to joints were extracted with eq.4

$$R_{joint}{}_{S2}^{S1} = (R_{S1}^{Earth})^T * R_{S2}^{Earth} \quad (4)$$

In which, for knee joint, S1 was the sensor placed on the thigh and S2 the sensor placed on the shank, while for ankle joint S1 was the sensor placed on the shank and S2 the sensor placed on the foot.

The elements inside R_{joint} were known, so with Euler convention YXZ [19] ,shown in eq.5, in which c is cosine, s is sine and x, y and z are the orientation axes of knee angles, it was possible to calculate the Roll (eq.6), Pitch (eq.7) and Yaw (eq.8) angles.

$$\begin{bmatrix} r_{00} & r_{01} & r_{02} \\ r_{10} & r_{11} & r_{12} \\ r_{20} & r_{21} & r_{22} \end{bmatrix} = \begin{bmatrix} c_y c_z + s_x s_y s_z & c_z s_x s_y - c_y s_z & c_x s_y \\ c_x s_z & c_x c_z & -s_x \\ -c_z s_y + c_y s_x s_z & c_y c_z s_x + s_y s_z & c_x c_y \end{bmatrix} \quad (5)$$

$$Roll = \text{asin}(-s_x) \quad (6)$$

$$Pitch = \text{atan2}(c_x s_y, c_x c_y) \quad (7)$$

$$Yaw = \text{atan2}(c_x s_z, c_x c_z) \quad (8)$$

Roll, pitch and yaw angles correspond to Abduction/Adduction angle, Flexion/Extension angle and Internal/External rotation angle.

The results obtained with this analysis are shown in section 3.2.1.

The main problem of this algorithm was the presence of electro-magnetic interferences during experimental trials, as PC's, treadmill etc., that affected data collected from magnetometers and produced errors in knee and ankle angles extractions.

In order to eliminate the dependence of data acquired from magnetometers, a new version of the algorithm, based only on accelerometers and gyroscopes data, was implemented and it will be explained in next section.

2.2.2.2. Integration of gyroscopes and accelerometers

The second version implemented was based on the integration of data acquired from gyroscopes and accelerometers, in order to avoid electro-magnetic interferences with magnetometers. Sensors located on thigh and shank were used to calculate knee angles while sensors located on shank and foot were used for ankle angles.

The algorithm was divided in 3 parts. The first calculated angles through accelerometers data, the second calculated angles through gyroscopes data and, in the third part, is shown the integration of these data.

Signals acquired from accelerometers, located on thigh, shank and foot, were filtered with a second order Butterworth low pass filter with a cut off frequency of 1.5 Hz.

Two bi-dimensional vectors containing the accelerations in the X and Z planes were created in order to have acceleration vector in sagittal plane, for each segment considered as shown in figure 15.

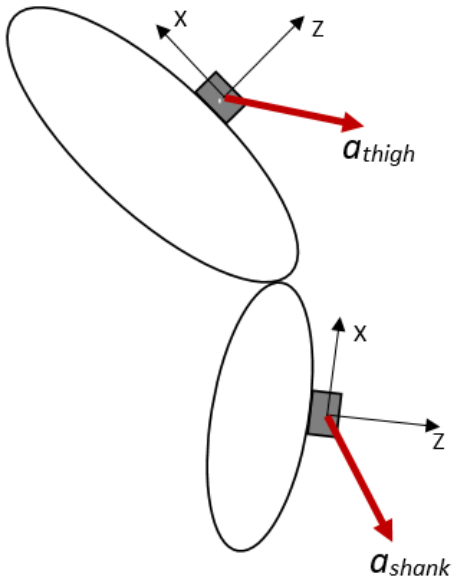

Fig.15. The image shows acceleration vectors of thigh and shank in the sagittal plane.

Knee and ankle angles were then calculated as the arc-cosine of the dot product of, respectively, thigh and shank sagittal vectors and shank and foot sagittal vectors divided for the product of their norm, multiplied by 180/π in order to convert from radiant to angles, as shown in eq.9.

$$Acc\_Angle = acos\ \frac{Acc_ySeg_1 * Acc_ySeg_2}{norm(Acc_ySeg_1)norm(Acc_ySeg_2)} * 180/\pi \quad (9)$$

where Acc_ySeg_1 and Acc_ySeg_2 are the accelerations, in the sagittal plane, of thigh and shank used to calculate knee angles and of shank and foot used to calculate ankle angles.

In the second part of the algorithm angular velocities from thigh, shank and foot were acquired and then filtered with second order Butterworth high pass filter with a cut off frequency of 5 KHz, in order to obtain filtered angular velocities of body segments, in each plane.

The angular velocities of joints were then obtain as the difference, respectively, of thigh and shank angular velocities for knee and the difference of shank and foot angular velocities for ankle (eq.10) where $AngVelSeg_1$ is the angular velocity of proximal body segment and $AngVelSeg_2$ is the angular velocity of distal body segment. Referring to the knee, $AngVelSeg_1$ correspond to the angular velocity of the thigh, and $AngVelSeg_2$ is the angular velocity of the shank, whereas for the ankle they correspond, respectively, to the angular velocities of the sank and of the foot. These signals were then integrated and multiplied by a constant value , 180/π*0.02, in order to change from radiant to degrees, as shown in eq.11.

$$JointAngVel = AngVelSeg_1 - AngVelSeg_2 \quad (10)$$

$$Gyro\_Angle = \sum_{first\ step}^{last\ step}(JointAngVel) * \frac{180}{\pi} * 0.02 \quad (11)$$

The angles calculated were affected by a drift due to integration of angular velocities. In order to remove the drift an integration of accelerometers data and gyroscopes data was applied. For each leg, during stance phases, knee and ankle angles were extracted from accelerometers data, whereas during the rest of the stride, angles were calculated from data extracted from gyroscopes, to which was summed the last value of angle calculated, in order to have integration.

The algorithm was validated offline, using Matlab (Mathworks, United States), on gyroscopes and accelerometers data acquired during experimental trials of 3 minutes walking with changes in direction and velocity. The results obtained will be shown in section 3.2.2.

2.2.2.3. Detrended gyroscopes

In the third version of the kinematics, knee and ankle angles were extracted from gyroscopes data as shown in the previous section. In order to remove the drift due to integration of angular velocities, a different algorithm was implemented. Data acquired from experimental trials showed that the drift, inside a single stride, followed a linear trend. The algorithm calculated the slope of the trend during a stride and used this value to correct the drift in the next stride. In this way all the strides were “detrended”, except for the first step.

The algorithm was validated offline, using Matlab, on data acquired from gyroscopes, under the same conditions explained in section 2.2.2.2. The results obtained will be shown in section 3.2.3 in which there will be also a comparison between the last two algorithm in order to choose the one that better remove the drift due to integration of gyroscopes.

2.2.3. Iterative Learning Controller

An Iterative Control Learning (ILC) algorithm was developed to control the neuroprosthesis. This method allows to control knee and ankle angles from the preparation of the swing phase to the detection of the MS event (phases 4 and 5 of the state machine featured in figure 13), in order to obtain a walk, in terms of kinematic, similar to a healthy subject.

On a previous study, concerning the improvement of a limited ability to dorsiflex the foot (droop-foot) [20], Seel et al. used an algorithm for inertial sensor-based foot-to-ground angle measurement and three electrodes, to stimulate the tibialis anterior muscle and peroneal nerve, that innervates the fibularis longus muscle. To drive the stimulation, an iterative learning controller, that uses step-by-step learning to reach desired eversion foot-to-ground angles, was implemented.

In this work, to deliver electrical stimulation, four electrodes (see hardware section), placed on right leg, are used. Two stimulate the gastrocnemius, in order to have knee flexion and the other two, through the stimulation of tibialis anterior muscle, cause ankle's dorsiflexion in order to correct the involuntary plantar-flexion of the foot, induced by the gastrocnemius muscle.

To compare all the signals acquired from all the sensors, a reference trajectory was extracted calculating the mean value of the trajectories acquired during phases 4 and 5 from twelve subject, age: 24.8 ± 1.3 years, height: 1.73 ± 0.11 m, weight: 60.8 ± 11.4 kg, on a walking straight trial at normal speed, for both knee and ankle. All the trajectories obtained during these phases were then remapped on 100 samples, using an off-line algorithm on Matlab, in order to have the same length. Through a statistical analysis, the mean values of gait phases 4 and 5 remapped and the standard deviation were calculated in order to have a mean trajectory and the variability for healthy subjects. Since reference signals had a constant length of 100 samples, also knee and ankle angles acquired during experimental trials, were remapped, in order to calculate the error, frame by frame, between references and trajectoris of knee and ankle. The remapping was made by calculating a cubic spline, that

used, as nodes, values of the trajectory recorded from the sensors and then remapped on 100 samples. To calculate the cubic spline the following equation was used:

$$S_i(x) = a_i + b_i(x - x_i) + c_i(x - x_i)^2 + d_i(x - x_i)^3 \quad (12)$$

Where:

$$a_i = y_i \quad (13)$$

$$b_i = -\frac{h_i}{6} z_{i+1} - \frac{h_i}{3} z_i + \frac{y_{i+1} - y_i}{h_i} \quad (14)$$

$$c_i = \frac{z_i}{2} \quad (15)$$

$$d_i = \frac{z_{i+1} - z_i}{6h_i} \quad (16)$$

The parameters h and b were could be calculated as:

$$h_i = x_{i+1} - x_i \quad (17)$$

$$b_i = \frac{y_{i+1} - y_i}{h_i} \quad (18)$$

Through the Gaussian elimination, u and v were found as:

$$u_1 = 2(h_0 + h_1) \quad (19)$$

$$v_1 = 6(b_1 - b_0) \quad (20)$$

$$u_i = 2(h_{i-1} - h_i) - \frac{h_{i-1}^2}{u_{i-1}} \quad (21)$$

$$v_i = 6(b_i - b_{i-1}) - \frac{h_{i-1} v_{i-1}}{u_{i-1}} \quad (22)$$

With the Back-Substitution it was possible to calculate *z:*

$$z_n = 0 \quad (23)$$

$$z_i = \frac{v_i - h_i z_{i+1}}{u_i} \quad (24)$$

$$z_0 = 0 \quad (25)$$

Once that the trajectories were remapped, the core of the ILC was developed. The algorithm applied a time-dependent input trajectory at every step [20], as shown in eq.26:

$$u_{j+1} = sat_0^1\left[u_j + \lambda * (ref - e)\right] \quad (26)$$

in which *u* is the control variable, *j* is the number of step, λ is a vector of values of 100 samples, initialized to a constant value equal to 0.5 [20], *ref* is the reference trajectory and *e* is the error. To avoid the divergence of the control variable, that control the electrical stimulation, is saturated between zero and one.

The error was calculated as the cubic root of the difference, frame by frame, between reference and trajectory, in order to maintain sign information and because it gave more weight to large angles [19], as shown (eq. 27):

$$e = \sqrt[3]{reference - trajectory} \quad (27)$$

To control the stimulation, two variables, q_{gastro} and q_{tibial}, that represent the stimulation profiles given, respectively, to the gastrocnemius and to the tibialis anterior, were introduced and they were normalized by the individual maximum values tolerated. The profile of stimulation given to the gastrocnemius, in order to generate knee flexion was calculated as shown in eq.28:

$$q_{gastro} = u_{knee} * MAX\_PW \quad (28)$$

Where MAX_PW is the maximum value of pulse width set before the start of the trial.

By stimulating the gastrocnemius, due to its bi-articular nature, beyond knee flexion, also an involuntary plantar flexion of the foot was generated. In order to compensate this effect and to improve the range of dorsiflexion of the foot, limited by the pathology, the tibialis anterior

was stimulated, with a stimulation profile q_{tibial} calculated as shown in eq.29, to obtain dorsiflexion of the foot

$$q_{tibial} = (u_{knee} + u_{ankle}) * MAX\_PW \quad (29)$$

The aim of these two stimulation profiles was to generate a pattern of walking closer to the physiological values, during the gait phases of interest.

In figure 17 it is featured a flow diagram that summarizes the way in which the controller worked.

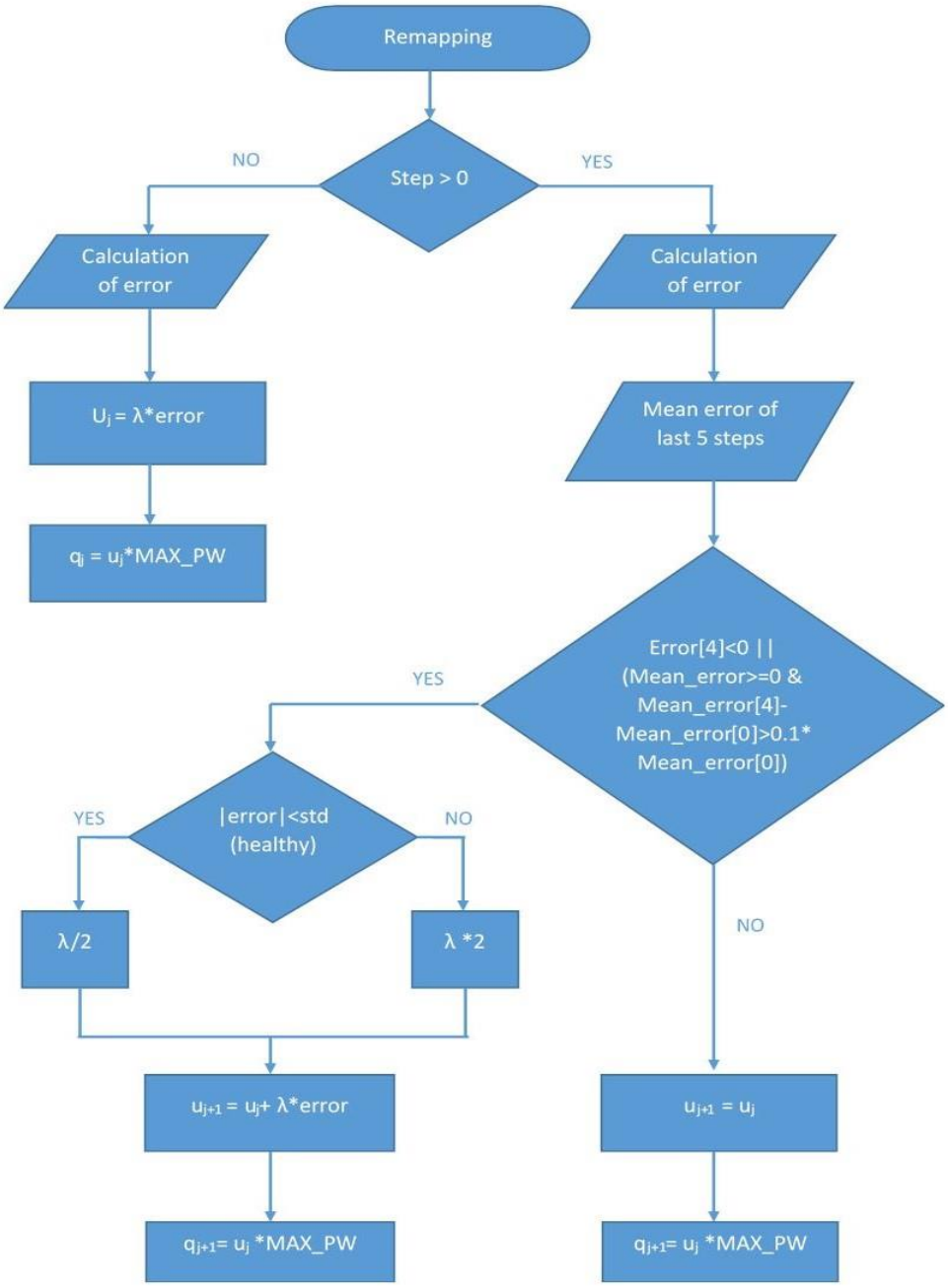

Fig.17 In the flow diagram is explained the way in which the ILC works

Trajectories of knee and ankle angles, extracted from the beginning of left double support phase to the detection of the mid swing of the right leg, were remapped on a constant length

of 100 samples, as the references. The algorithm then evaluated if the variable *step* was equal or greater than zero. If the first condition occurred, the error was found as shown in eq.27 and the control variable *u* was calculated as the product of the vector λ multiplied by the error.

The stimulation profile *q* was found, for the gastrocnemius and the tibialis anterior, as explained in eq.28 and eq.29.

If the variable *step* was greater than zero, the algorithm estimated the error and the mean values of the errors during the last five steps.

In this case, the control variable *u* was found in two different ways:

- If the last value of the mean error of the last step was lower than zero, or the values of the mean errors during the last five steps were greater or equal to zero and the difference between the last and the first mean errors was greater than the 10% of the mean value of the error at the first step, *u* was calculated with eq.26. The values inside the vector λ could change in respect to the absolute value of the error, compared to the mean standard deviation of the trajectories analyzed. If the error was lower than the mean value of the standard deviation of the reference, lambda was divided by two, otherwise it was multiplied by two.
- In the other case, the value of the control variable *u* remained constant for the following five steps, in order to avoid useless increase in stimulation intensity and the arise of muscles fatigue, when values of trajectory were greater than the preset reference or when improvements in trajectory between first and fifth step were not greater enough.

The stimulation profile *q*, in both cases, was found as shown in eq.28 and eq.29.

After a preliminary test, the algorithm was converted in C language in order to be used during online experimental trials. Results obtained will be shown in section 3.3.

The robustness of the neuroprosthesis was validated on 7 healthy subjects performing three different tasks, as explained in this section, through a one way Anova statistical analysis, in order to verify if the mean values of the stimulation profiles, for both gastrocnemius and

tibialis anterior, calculated during one task, were statistically different from the mean stimulation profiles computed during the other two tasks.

Through this analysis it was possible to verify if the stimulation profiles given to the muscles of interest, significantly varied in response to the variation of the performances required to the subjects. The results obtained from the validation will be shown in section 3.3.

2.3. Experimental setup

The experimental set-up used during acquisitions was composed of five inertial sensors, three placed on the right leg and the other two on the left leg, in order to extract kinematic and gait events during walking. To provide stimulation four surface electrodes were used, two were placed on the gastrocnemius and the other two on the tibialis anterior muscle. The positioning of sensors and electrodes is shown in figure 18.

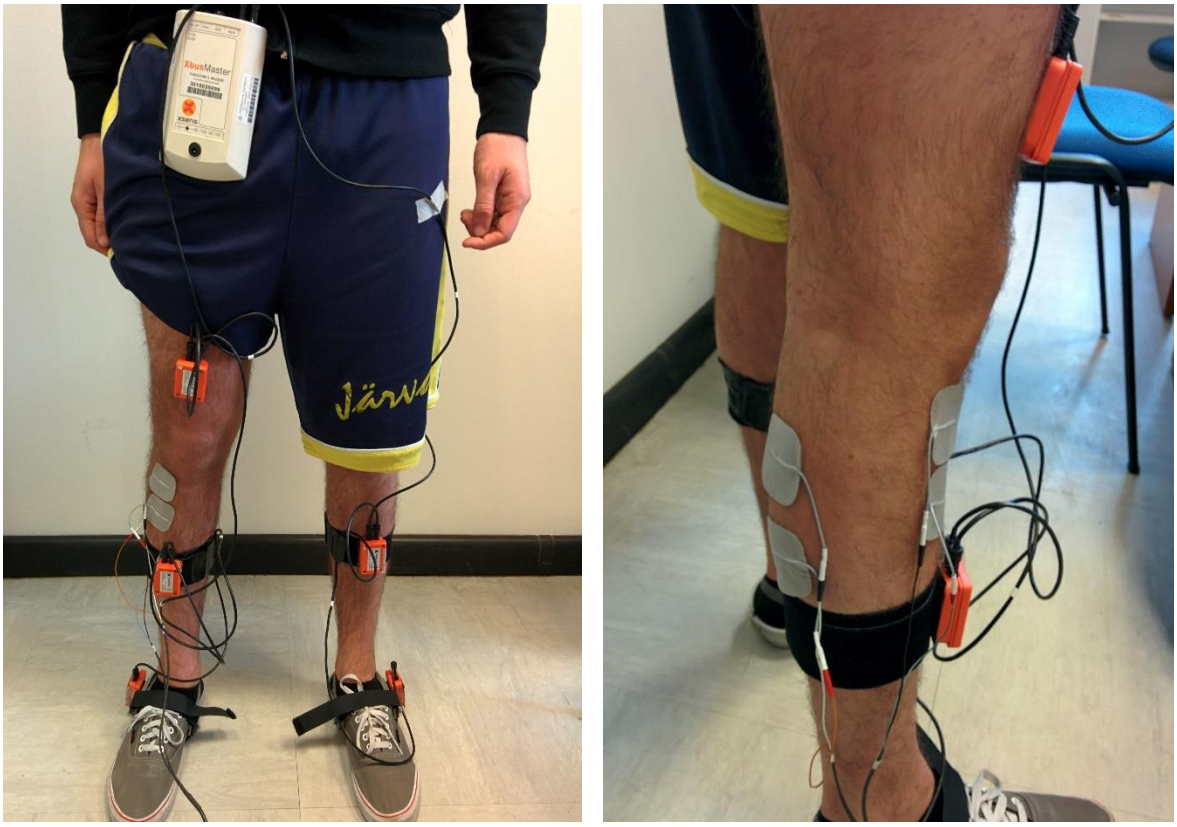

Fig.18. Experimental setup. Three sensors were placed on the right leg, one on the thigh, one on the shank and one on the foot. Two sensors were placed on the left leg, one on the shank and one on the foot. Four electrodes were placed on the right leg, two on the gastrocnemius and two on the tibialis anterior.

The robustness of the neuroprosthesis was evaluated on seven healthy subjects.

The experimental protocol used is the following. A calibration of intensity current of stimulation was performed, both for gastrocnemius and tibialis anterior muscle, the current was raised until the maximum value tolerated from each subject, the last value for each muscles was saved and the maximum current was set. The frequency of stimulation was set to 25 Hz in order to avoid muscular twitches and the maximum pulse width to 400 μs.

The subjects included in the study were asked to perform three different tasks. The first task consisted in normal walking at normal speed. During the first four steps of the trial, the calibration of the thresholds, necessary to detect gait events, was made.

During the second task was asked to the subject to walk changing their gait velocity, the same calibration file was used in this trial.

The third task consisted in walking with a reduced range of motion of knee and ankle joint in order to have values of trajectories far from the references calculated on healthy subjects.

3. Results

In this chapter are shown the results obtained from validation of real time detection real time detection algorithm, extraction of kinematic during walk, preliminary test and test of ILC controller.

3.1. Real-Time Detection

The improved Real Time Detection algorithm was validated in five different conditions as explained in section 2.2. The results obtained from these experimental trials are shown in figure 19.

For one repetition of every task requested, there is a comparison between detection of gait phases with the original version of the algorithm and the improved version of the same.

a)

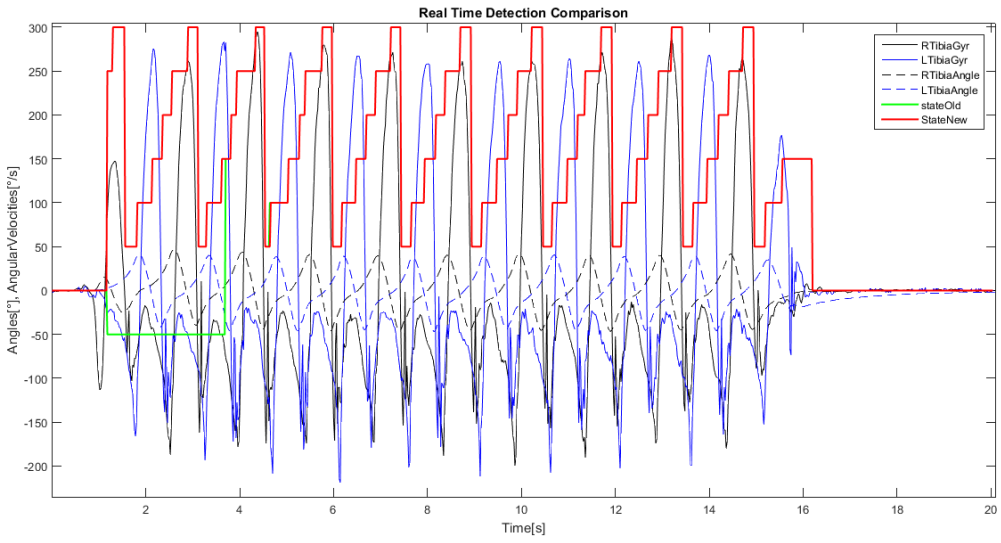

b)

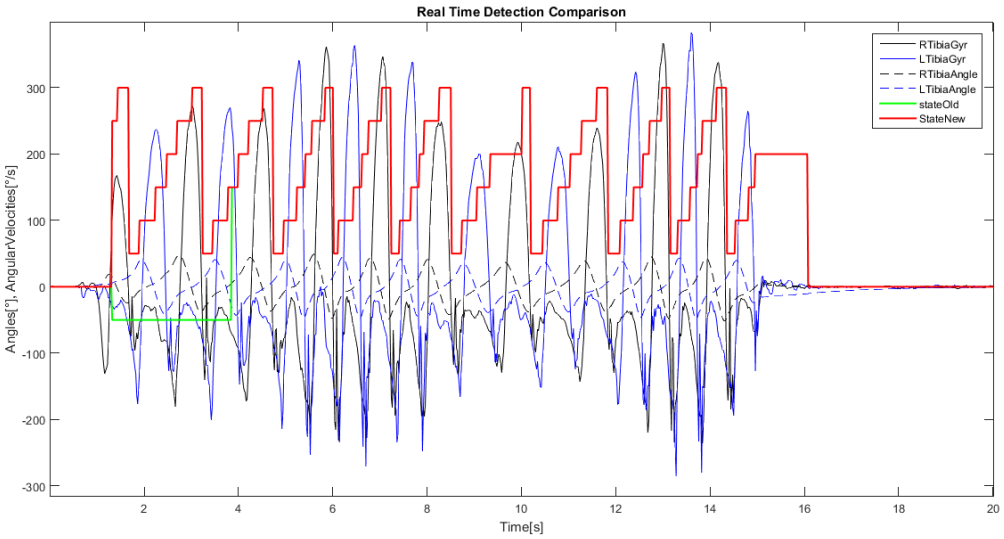
Real Time Detection Comparison
RTibiaGyr
LTibiaGyr
RTibiaAngle
LTibiaAngle
stateOld
StateNew
Angles[°], AngularVelocities[°/s]
Time[s]

c)

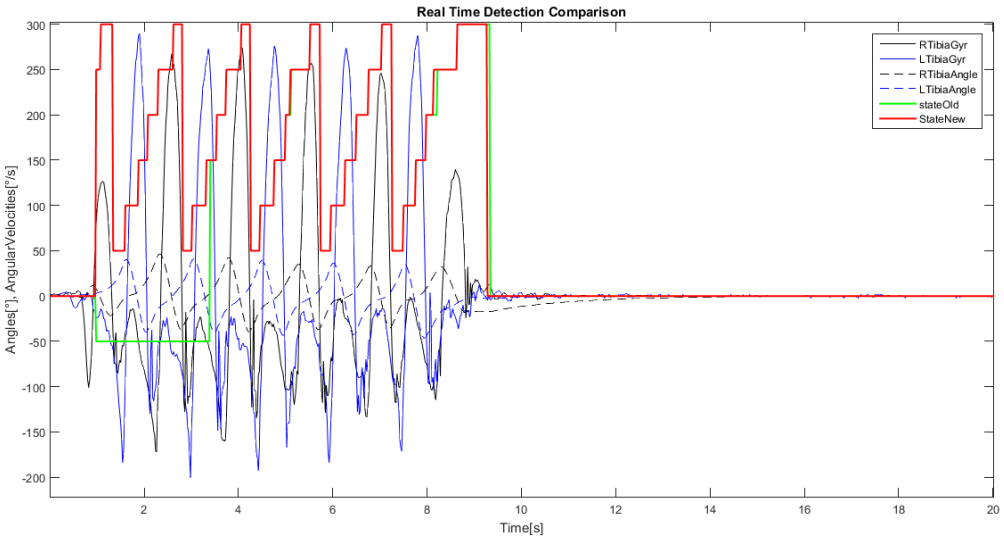
Real Time Detection Comparison
RTibiaGyr
LTibiaGyr
RTibiaAngle
LTibiaAngle
stateOld
StateNew
Angles[°], AngularVelocities[°/s]
Time[s]

d)

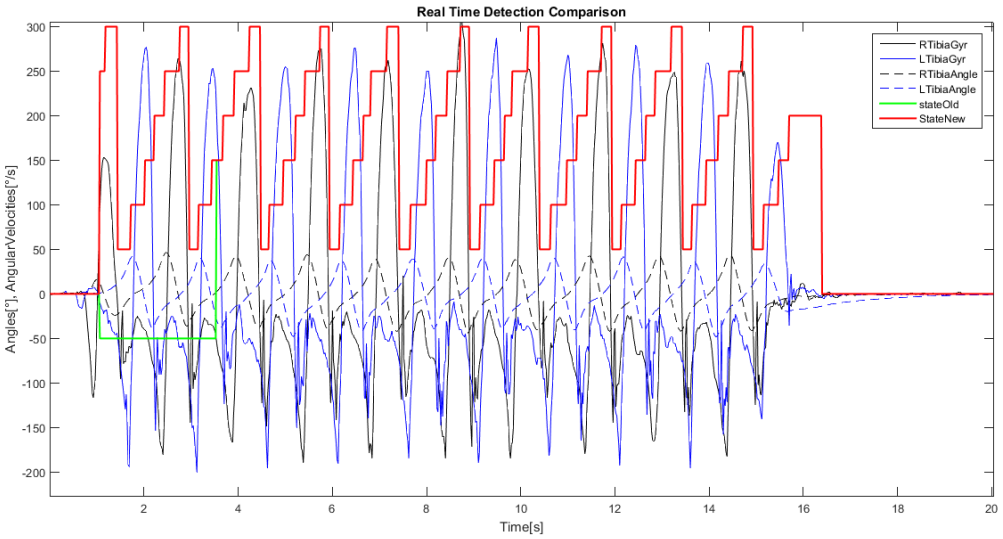

e)

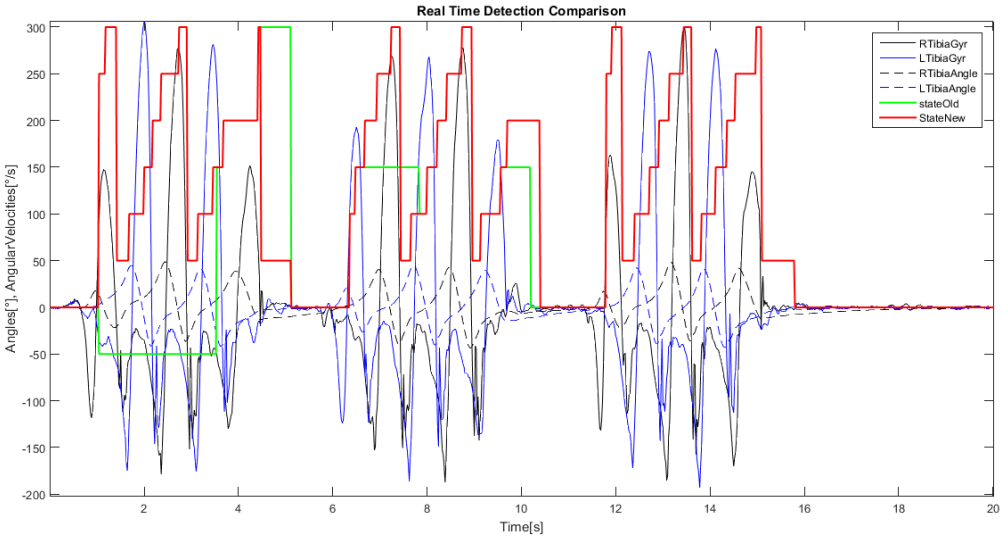

Fig.19. From panel a) to panel e) are shown results obtained during each task. On plots are displayed right and left shank angular velocities (black and blue lines), right and left shank angles (black and blue dashed lines) and state's value obtained from original algorithm (green line) and from improved algorithm (red line).

It can be seen that, for each task, the algorithm was able to correctly detect the six gait events (red lines in figure 19), from the first step. There was a perfect match between the detection of gait events computed by the original and the improved version of the algorithm and, in this particular repetition of the “start and stop” task, the last version of the algorithm detected gait phases better than the previous one. This improvement was very important because it offers the possibility to implement a controller, based on gait segmentation, able to work from the beginning of the trial, without making, four steps of calibration at the beginning of every trial.

The results obtained in terms of accuracy of the algorithm, assessed using the metrics Precision, Recall and F1-score, were calculated on 516 steps divided in the five tasks performed by the two healthy subjects (120 during task one, task two and task four, 66 during task three and 90 during task five), for a total of 1353 gait events.

The values obtained during the different tasks performed are shown in table 1.

Straight walking (N=354)	TP	354
	FP	0
	FN	0
	P	1
	R	1
	F1	1
Change in speed (N=360)	TP	351
	FP	0
	FN	9
	P	1
	R	0.9806
	F1	0.9902
Change in slope (N=198)	TP	195
	FP	0
	FN	3
	P	1
	R	0.9848
	F1	0.9923
Change in direction (N=348)	TP	345
	FP	1
	FN	2
	P	0.9971
	R	0.9942
	F1	0.9956
Start and stop (N=270)	TP	263
	FP	1
	FN	6
	P	0.9962

	R	0.9777
	F1	0.9827

Table.1.In the table are shown the results obtained from the accuracy analysis during the five task performed, repeated three times by each subject. N corresponds to the number of gait events occurred during each task. TP, FP, FN correspond to True Positive (gait events correctly detected), False Positive (events wrongly detected) and False Negative (events did not detected). P, R and F1 are the metrics referring to precision, recall and F1-score.

From the accuracy analysis of the metrics P, R and F1-score, very high value of precision, recall and F1-score were found during each task. The best results were obtained during straight walking for twenty steps. During the performance of this task, no FP or FN were detected and for this reason, as explained in eq.1, eq.2 and eq.3 the values assumed by the metrics were equal to one. Also in the other tasks performed the values of the metrics were really close to one. This means that, the improved algorithm, could detect gait events with a high accuracy, during different tasks, such as changes in velocity, changes in direction, changes in slope and start and stop trials.

3.2. Kinematic analysis

This section is divided into three paragraphs and shows results obtained for each algorithm used to extract kinematic during walking and the explanation of the algorithm used to pilot the Iterative Learning Controller.

The first algorithm was based on rotation matrices, the second one on integration of data collected from accelerometers and gyroscopes and the third one was based on correction of the drift induced by integration of angular velocities extracted from gyroscopes.

3.2.1. Rotation matrices

In figure 20 are displayed right and left knee angles, extracted during a 10 steps trial, with rotation matrices algorithm.

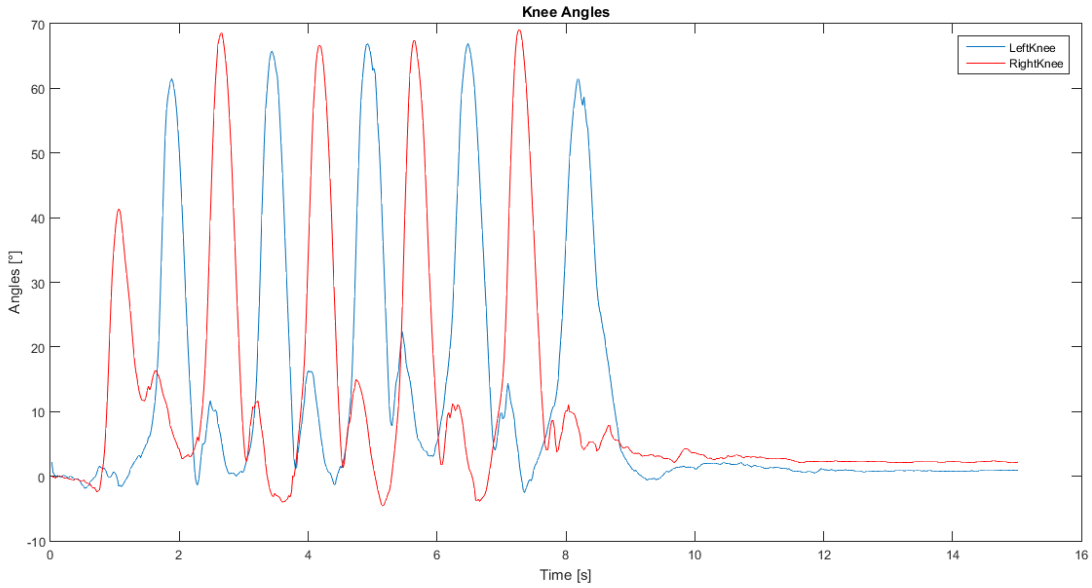

Fig.20. Flexion/Extension knee angles extraction with rotation matrices algorithms.

The algorithm worked properly during the whole trial. The reason that led to the choice of another kind of algorithm implementation was that the magnetometer measures were affected by electro-magnetical interferences, as PC's and treadmills, that induced errors in knee and ankle angles extraction, as discussed in section 2.2.1.

3.2.2. Integration of gyroscopes and accelerometers

The algorithm used accelerometers data in order to correct drift in gyroscopes data due to integration of angular velocities. The results obtained, for right and left knee, during a trial in which the subject performed three minutes walking at normal speed, are shown in figure 21.

a)

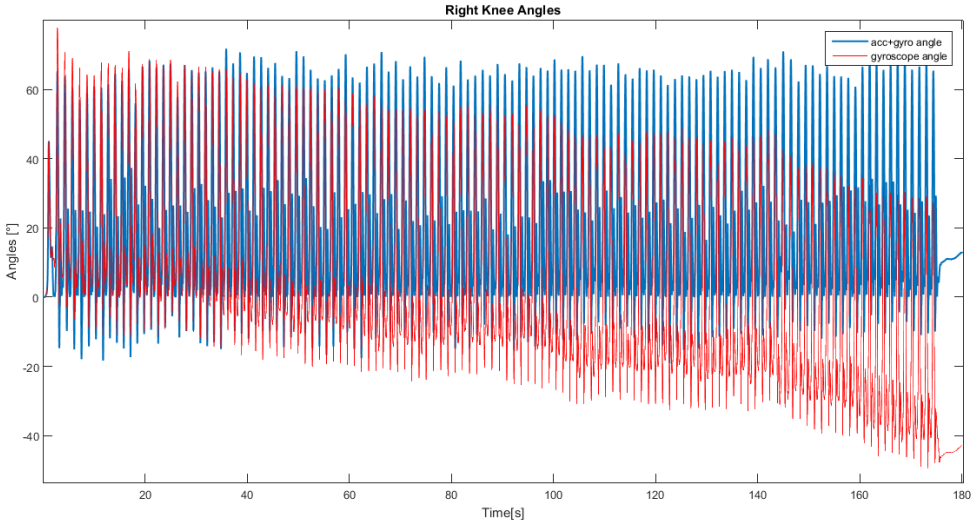

b)

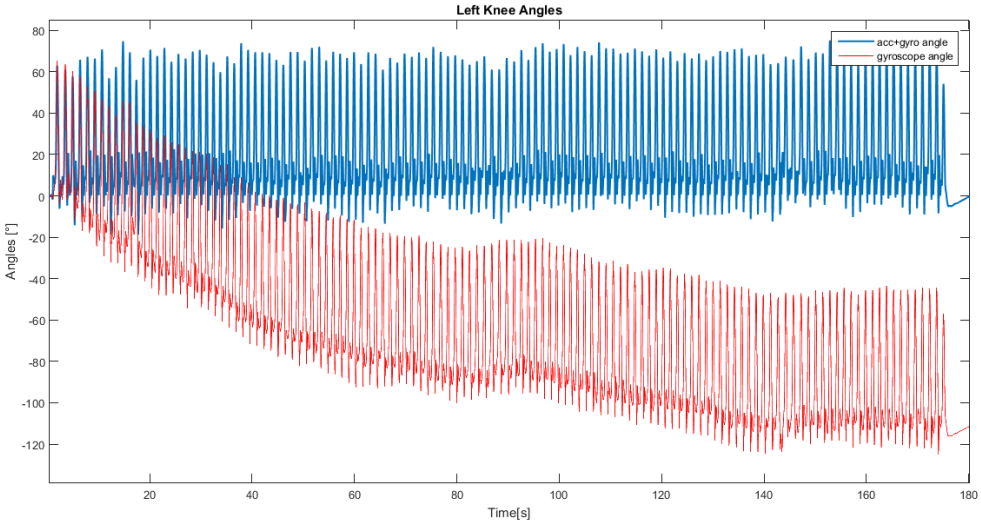

Fig.21. Panel a) shows right knee angles during 3 minutes walk trial. Panel b) shows left knee angles extracted in the same trial.

The drift obtained due to integration of angular velocities was corrected for both knees. However, as figured in panel “a”, right knee angles often assumed values lower than -10 degrees, which could not be representative of the kinematic of the joint. For this reason, another algorithm to correct the drift was implemented and the results obtained from its validation will be shown in the next section.

3.2.3. Detrended gyroscopes

From the experimental trials it was clear that the drift induced by integration of gyroscopes follows a linear drift in each stride. For this reason the main idea of the third version of the algorithm for kinematic extraction was to correct the drift in each stride with a “linear detrend”. The results obtained from an offline analysis via Matlab, of data already acquired, were better than the one obtained with the previous versions. After this validation the algorithm was converted in C language and tested during a three minutes walking trials. Figure 22 shows, for right and left knees, the results obtained during the trial.

a)

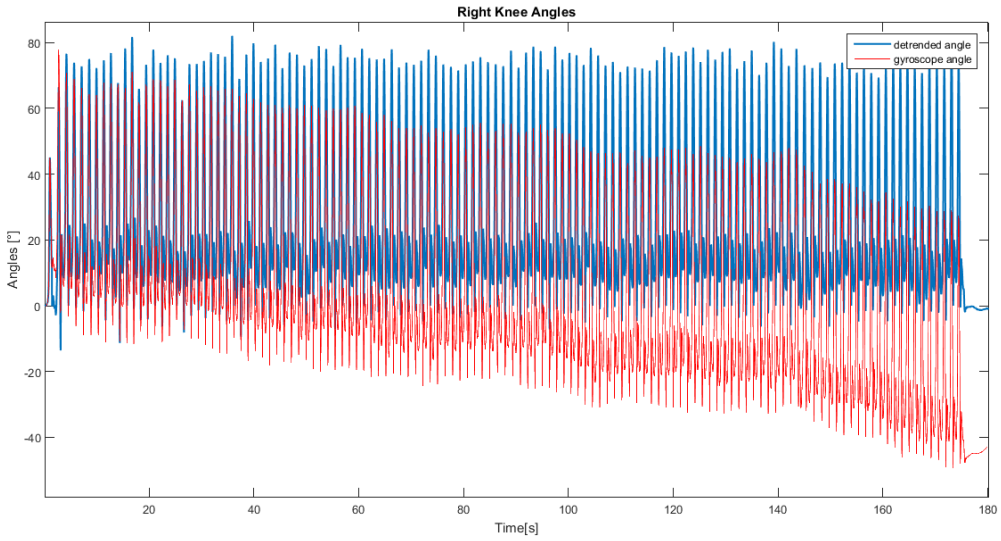

b)

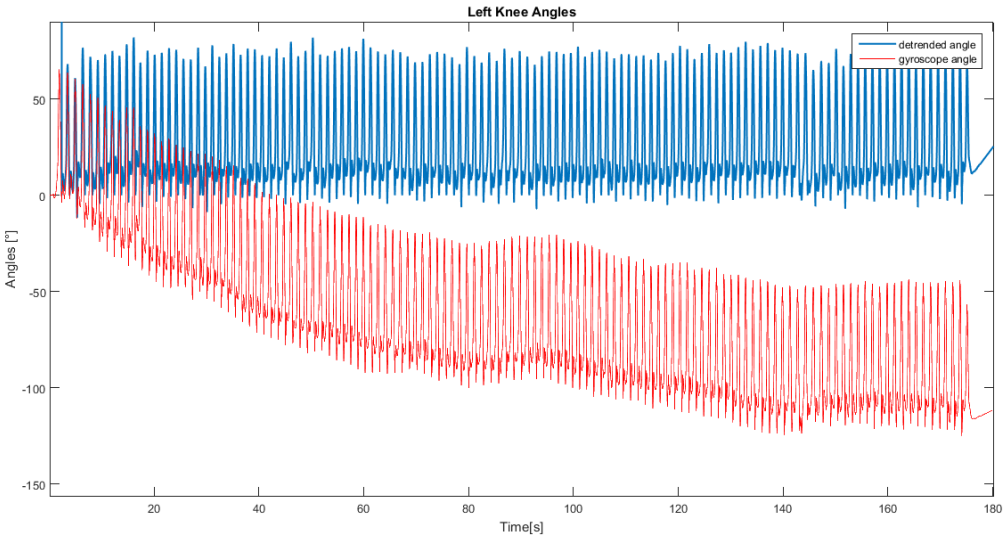

Fig.22. Panel a) shows right knee angles during 3 minutes walking trial. Panel b) shows left knee angles extracted in the same trial.

For both knees the drift was corrected. From figure 19a it is clear that the algorithm worked better than the one based on integration of accelerometers and gyroscopes data, because knee angle assumed, as minimum peak, values closer to zero during the most of the trial, while in the previous version values minimum values was closer to -10 degrees.

Angles extracted with this version of the kinematic analysis were closer to physiological values than the results obtained with the second version of the kinematic analysis and were not influenced by electro-magnetical interferences as the rotation matrices algorithm. For these reasons, the algorithm was converted to C languages, in order to extract, during on-line trials, knee and ankle trajectories necessary to the ILC.

3.3. Iterative Learning Controller

In this section are shown the results obtained during the preliminary test of the ILC algorithm and the results obtained from the test of the neuroprosthesis during experimental trials.

Through the use of a cubic spline interpolation, trajectories extracted from the preparation of the swing phase to the detection of the MS event, were remapped on 100 samples, as shown in figure 23.

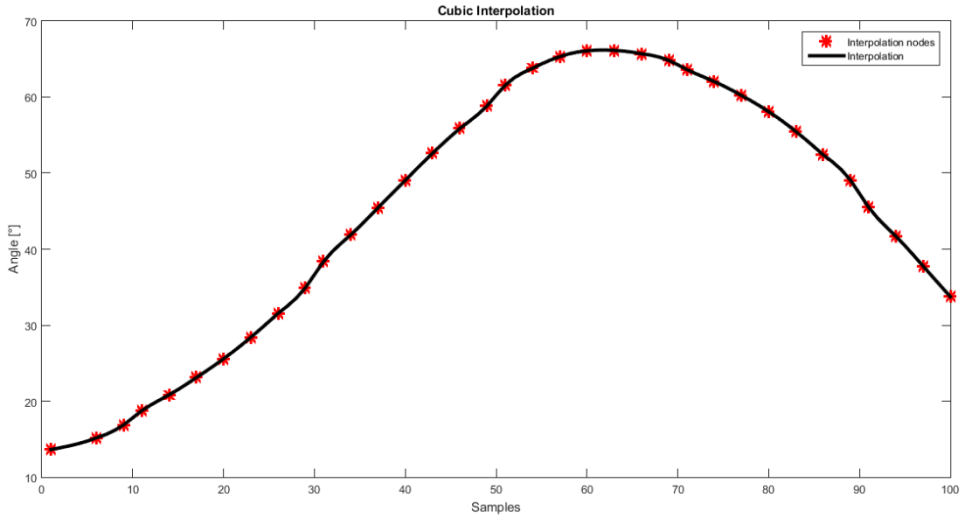

Fig.23. In figure is represented the cubic spline interpolation. The red stars correspond to the 35 samples of the original trajectory acquired and the black line correspond to the remapped trajectory of 100 samples.

After the remapping on 100 samples, two references, one for the knee and one for the ankle, were extracted, as explained in section 2.2.3, and the results obtained are shown in figure 24.

a)

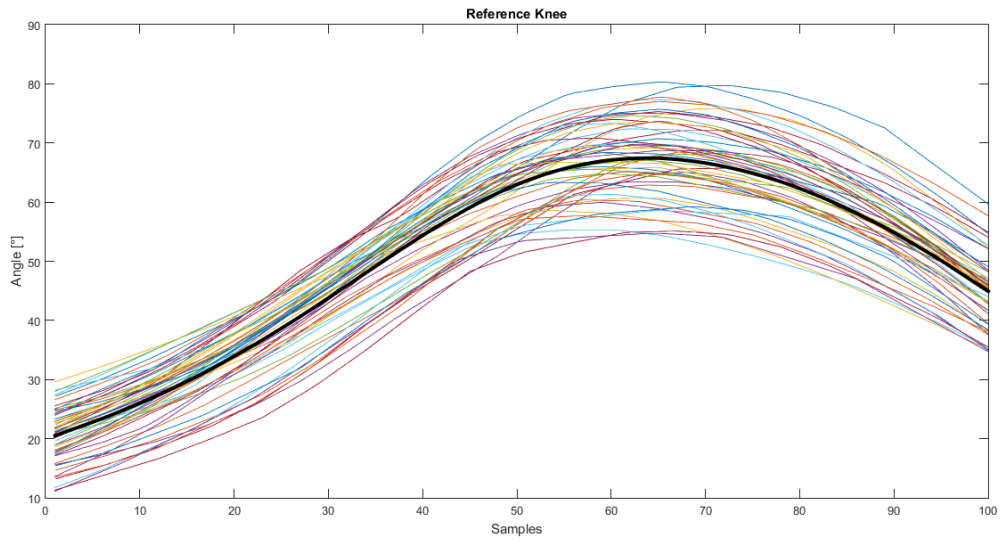

b)

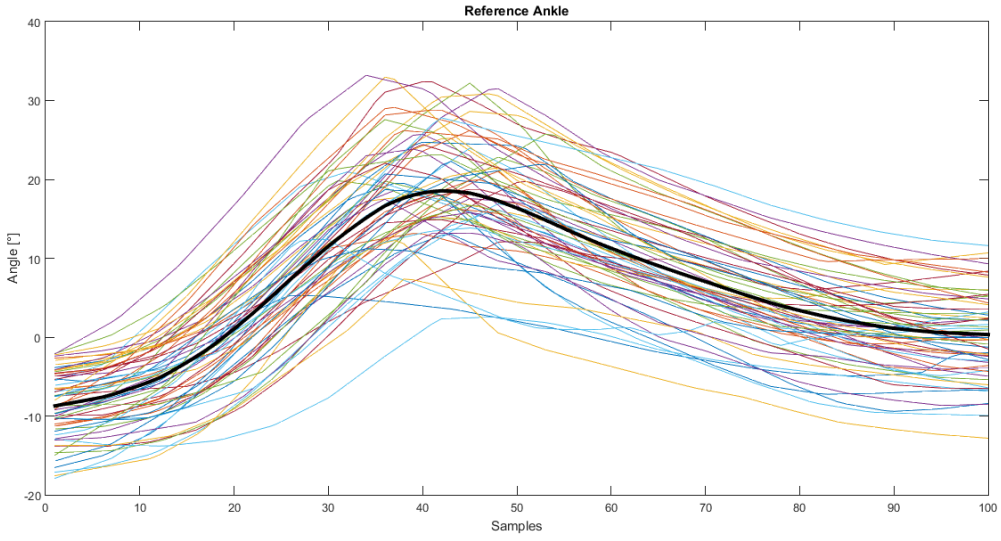

Fig.24 a) Knee trajectories acquired during gait phases 4 and 5 , in black the reference calculated as the mean value of all the trajectories b) Ankle trajectories acquired during gait phases 4 and 5, in black the reference calculated as the mean value of all the trajectories.

A statistical analysis was performed in order to obtain the mean variability of knee and ankle trajectories of healthy subjects during these phases. For this, the standard deviation of the angles was calculated and its mean value was kept as the representative angle variability throughout the phases considered before.

In figure 25 are shown the references of knee and ankle with their standard deviations.

The range of knee angle goes from 20.01 degrees to 40.21 degrees with a maximum peak of 67.87 degrees, with a mean value of standard deviation equal to 6.8533 degrees, whereas the range of ankle angle goes from -8.13 degrees to -2.53 degrees with a maximum peak of 18.54 degrees, with a mean value of standard deviation equal to 7.2659

a)

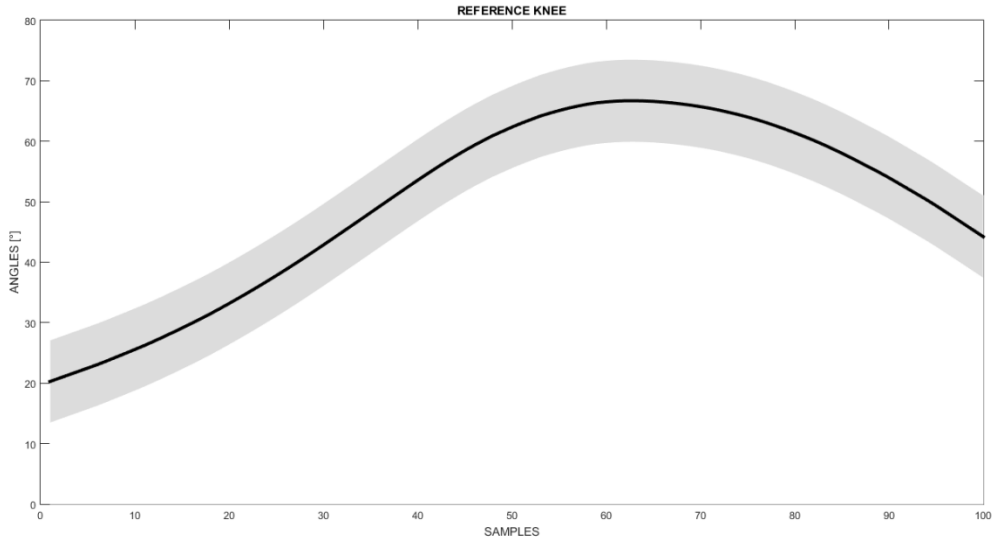

b)

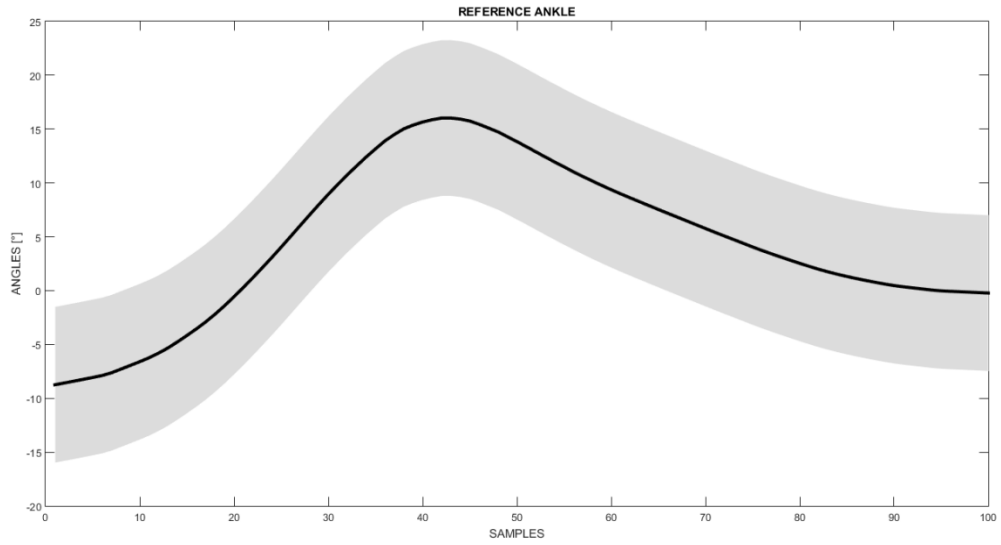

Fig.25. a) Knee reference (black line) with its range of variability (gray). b) Ankle reference (black line) with its range of variability (gray).

The algorithm was then tested offline, using Matlab. All the remapped trajectories, for both knee and ankle were set to zero and, as proposed by Seel at al., the value of the control variable *u* at the first step was set to zero[20].

From the second step the control variable increases until the saturation value, as featured in figure 26, where the amplitude of the control variable *u* is represented, for every step, as a function of the gait cycle.

a)

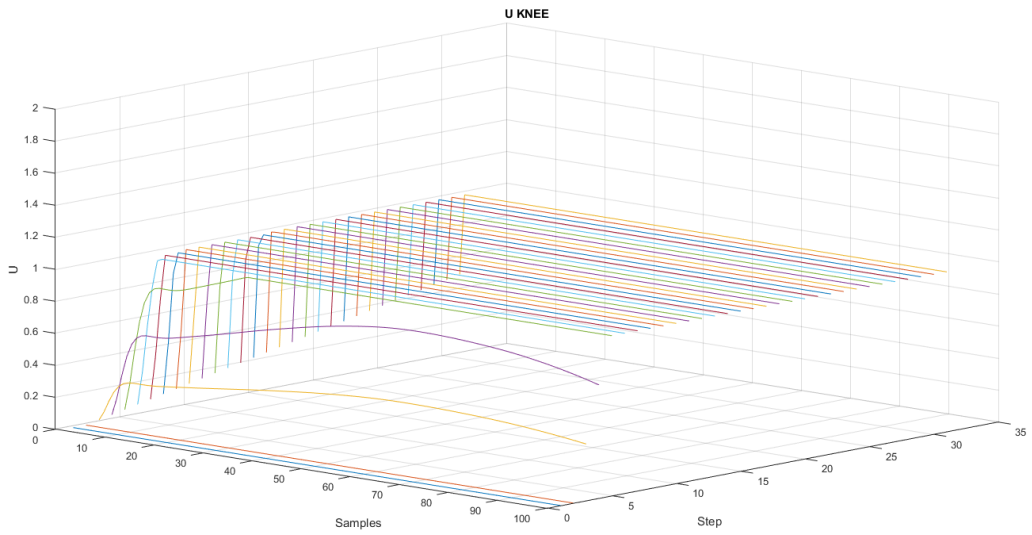

b)

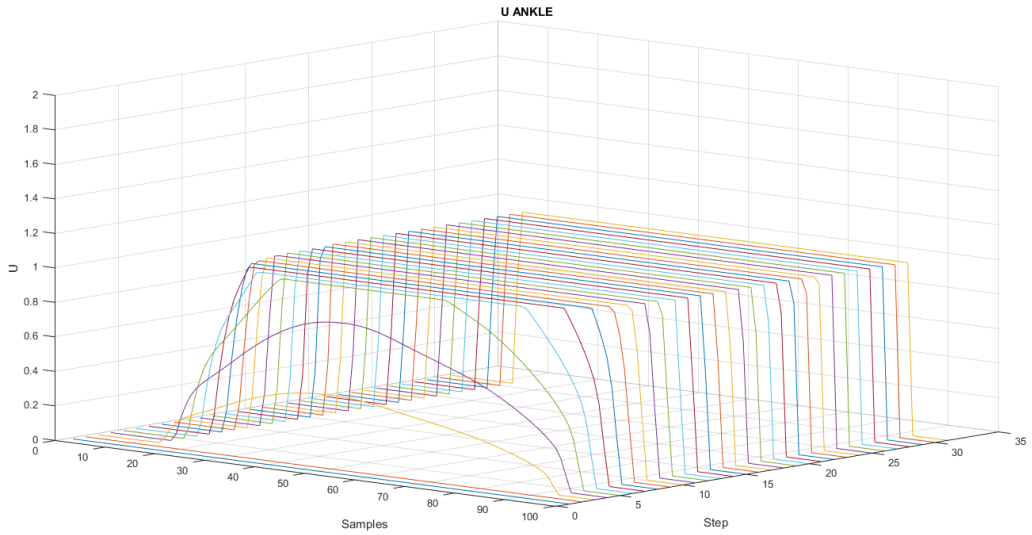

Fig.26. a) Distribution of stimulation of knee joint. After 3 steps the control variable reached the saturation value b) Distribution of stimulation of ankle joint. Due to the saturation to 0 for negative value of u, at the beginning of gait phase 4 and at the end of gait phase 5 the control variable Is equal to 0.

Figure 26a shows that after three steps, the control variable *u* reached the value of saturation, whereas figure 26b shows that distribution of stimulation of the ankle is equal to zero at the beginning and at the end of the gait phases analyzed, while it is equal to one in the middle. This is caused by the fact that trajectories, at every steps, were set to zero, so the error and *u* were lower than zero. As explained in section 2.2.3 if the value of the control variable is lower the zero it is saturated to zero.

After a preliminary test of the ILC algorithm, the neuroprosthesis was tested on-line on seven healthy subjects, as explained in section 2.2.4. The results obtained during the different tasks performed by one subject are here represented. The comparison between the references and the trajectories acquired during the first task, is shown in figure 27.

a)

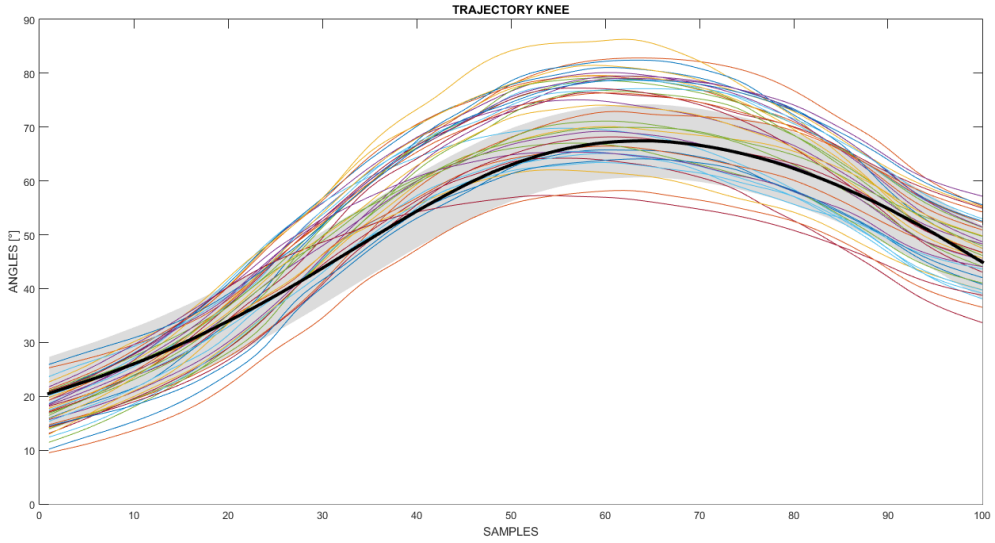

b)

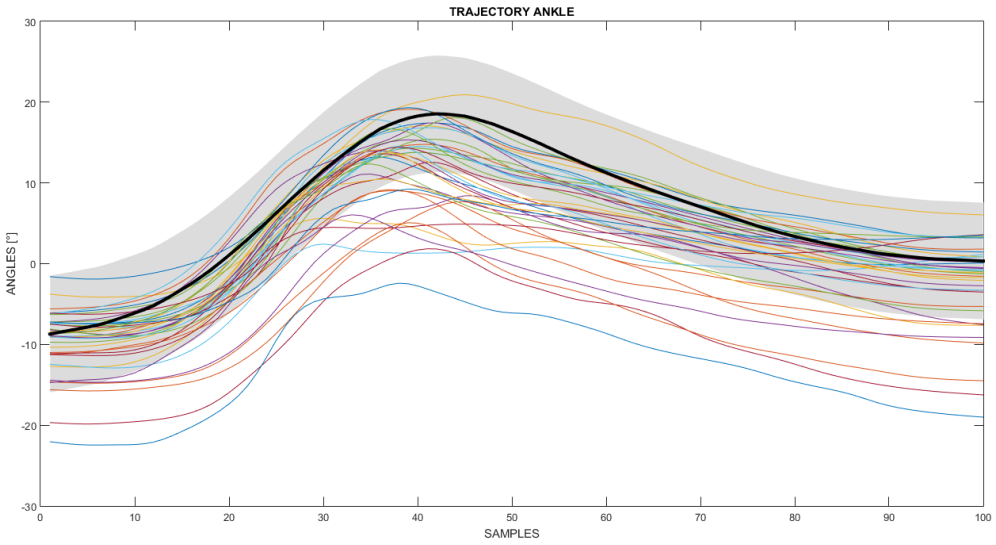

Fig.27. In panel a and panel b are shown the comparisons between references (black lines) of knee and ankle, with their standard deviations (gray), and the trajectories acquired during phases of interest.

It can be seen that knee trajectories were often higher than the reference, whereas, referring to ankle joint, trajectories were lower than the reference.

The results obtained, in terms of distribution of stimulation *u* are shown in figures 28.

a)

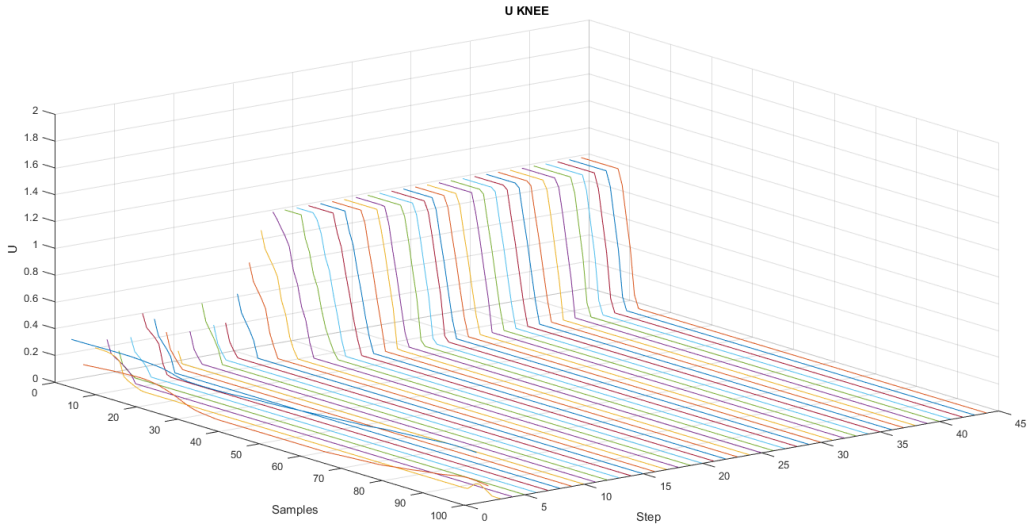

b)

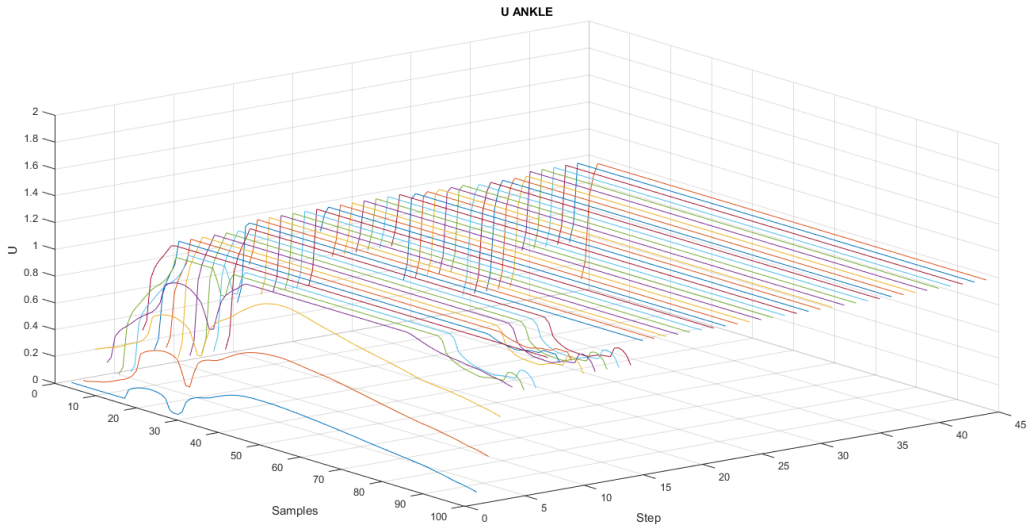

Fig.28. The figure shows the variations of the control variable, both for knee (panel a) and ankle (panel b).

The results shown in figure 28 match with the results featured in figure 27.

Knee distribution of stimulation assumed values greater than zero when trajectories were lower than the reference, while, when trajectories were higher than the reference, it was equal to zero.

Referring to the ankle, for the most of the trial, the distribution of stimulation reached the saturation value, in fact trajectories acquired were often lower than the reference.

The stimulation profiles *q* obtained*,* calculated as the control variable *u* multiplied by the value of pulse width chosen (400 µs), are shown in figure 29.

a)

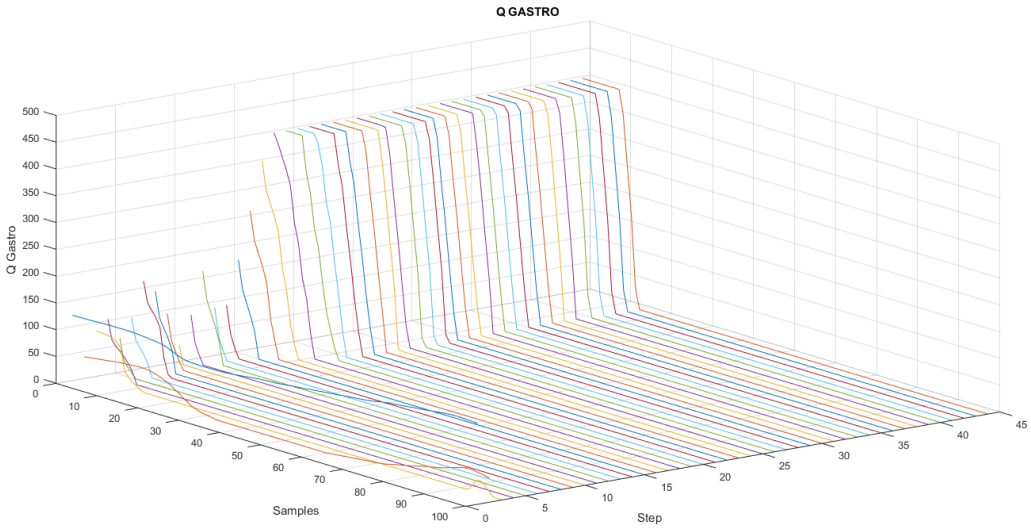

b)

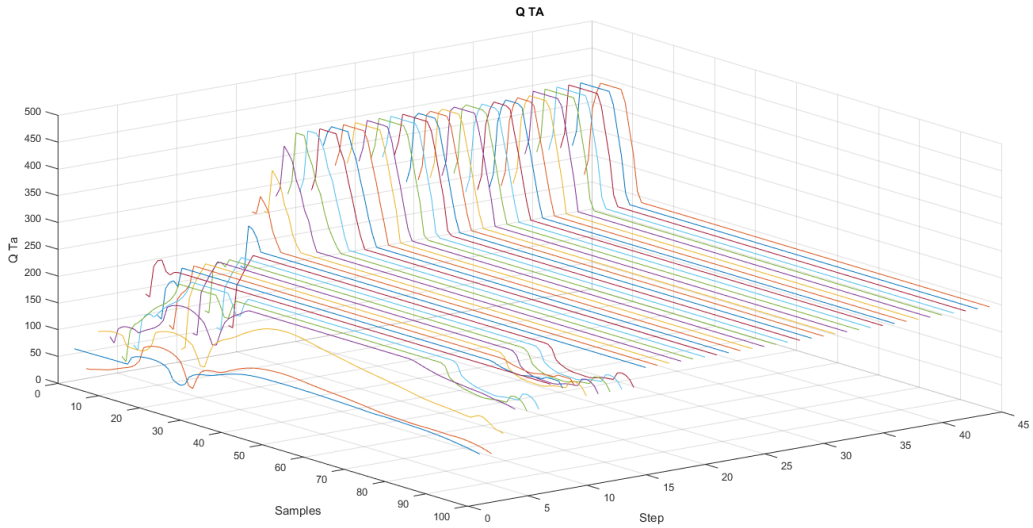

Fig.29. Stimulation profile given to the gastrocnemius (panel a) and to the tibialis anterior (panel b).

The stimulation profile given to the gastrocnemius corresponds to the value of the control variable u_{knee} multiplied by the pulse width, as explained in eq.25, whereas the stimulation profile given to the tibialis anterior corresponds to the sum of the control variable u_{knee} with the control variable $u_{ankle,}$ multiplied by the pulse width, as explained in eq.26.

Results obtained during the performance of the second task are shown in figure 30.

a)

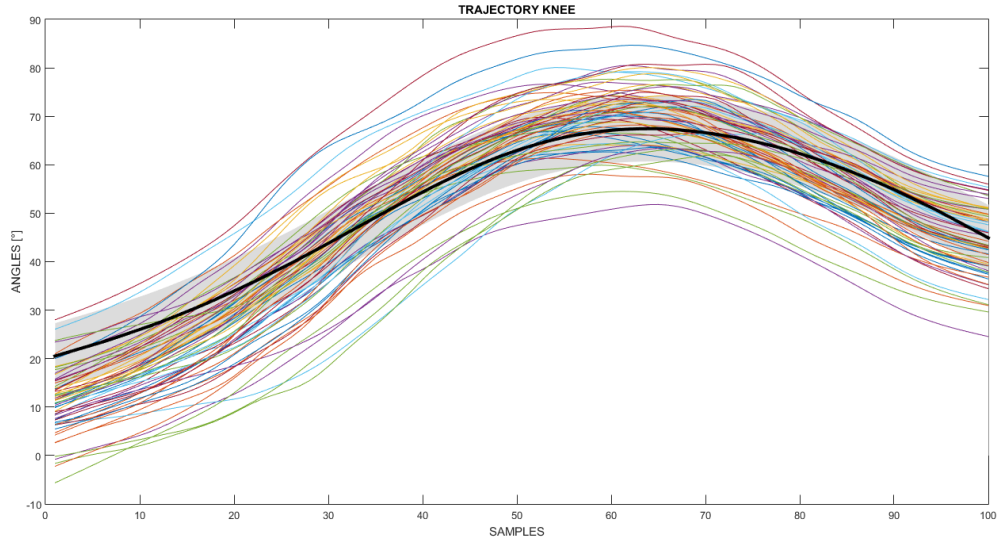

b)

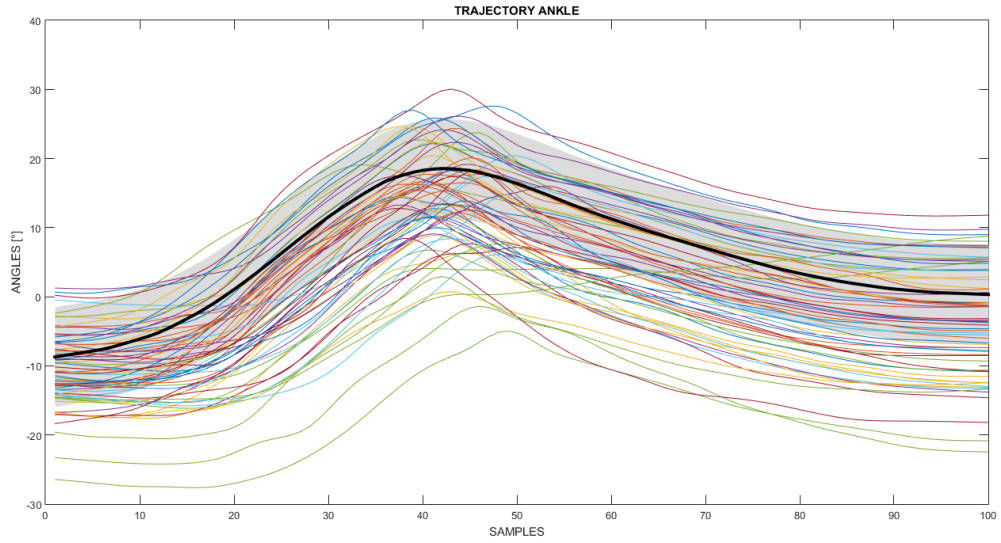

Fig.30. In panel a and panel b are shown the comparisons between references (black lines) of knee and ankle, with their standard deviations (gray), and the trajectories acquired during the different cycles.

Trajectories, for both knee and ankle, were often inside the range of variability. Referring to knee joint, trajectories, at the beginning of gait phase 4 and at the end of gait phase 5, were often lower than the reference, while they were higher in the middle, whereas, referring to ankle joint, trajectories assumed values often lower than the reference. The distributions of stimulation obtained during this trial are shown in figure 31.

a)

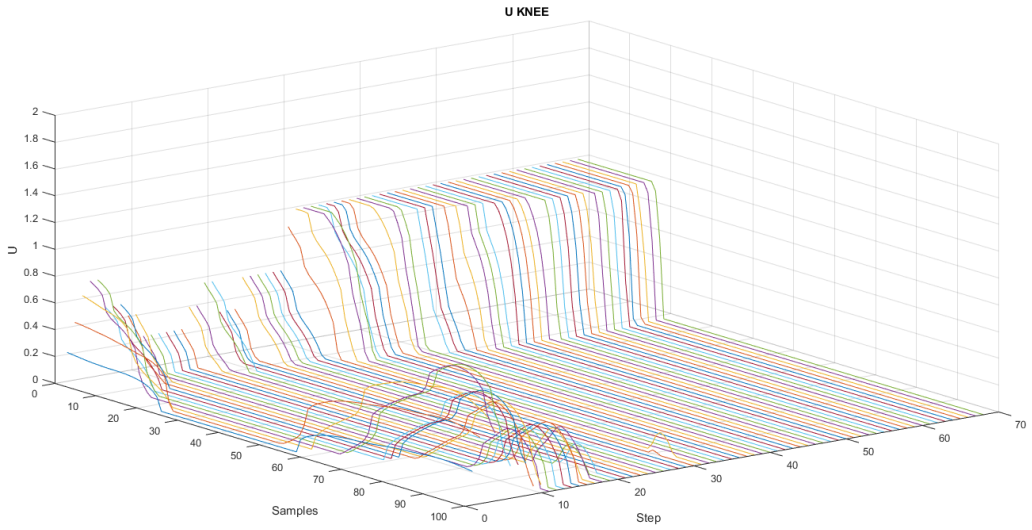

b)

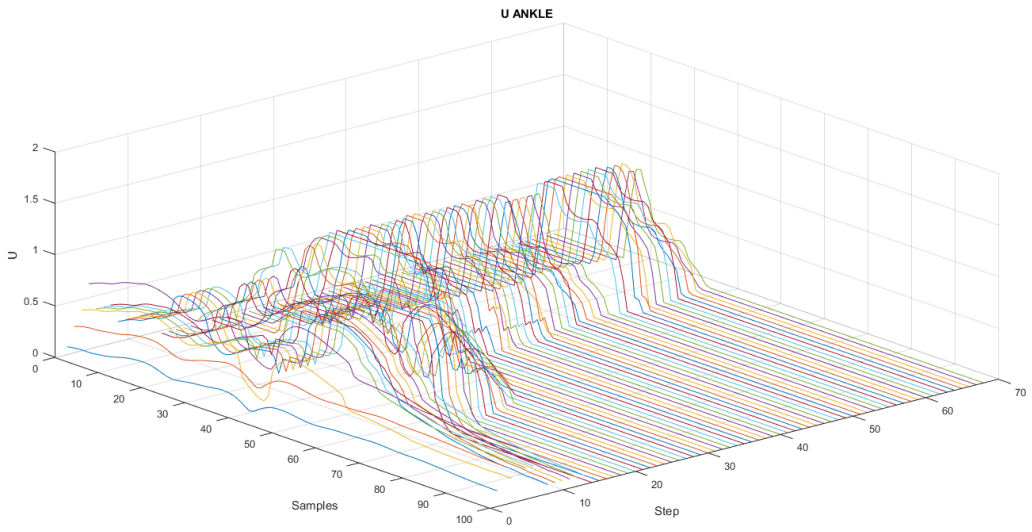

Fig.31. The figure shows the variations of the stimulation profile q, both for knee (panel a) and ankle (panel b).

For both knee and ankle, the distribution of stimulation assumed values greater than zero during the preparation of the swing phase, whereas it often decreased during the rest of the phases of interest, until it saturated to zero.

The stimulation profiles, for both gastrocnemius and tibialis anterior, related to these distributions of stimulation, are featured in figure 32.

a)

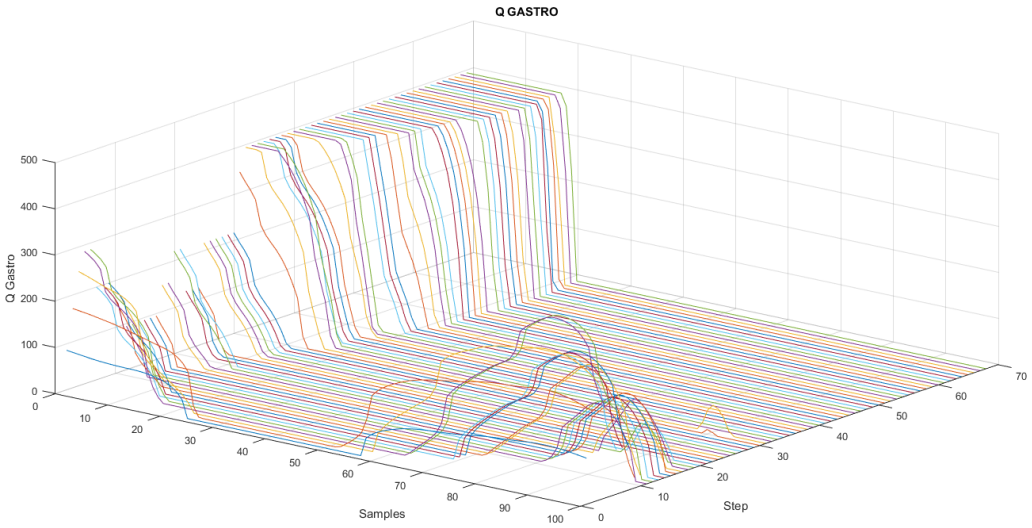

b)

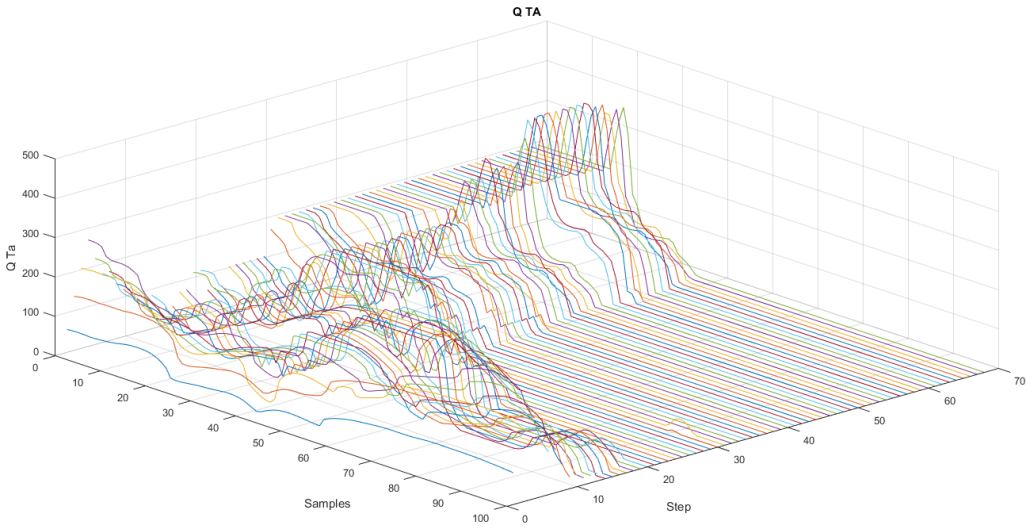

Fig.32. Stimulation profile given to the gastrocnemius (panel a) and to the tibialis anterior (panel b).

During the third task, which consisted in walking whit a reduced range of motion of knee and ankle joint, the results obtained were different, especially in terms of distributions of stimulation and stimulation profiles, from results obtained during the first two tasks. In figure 33 are shown trajectories of knee and ankle compared to the references.

a)

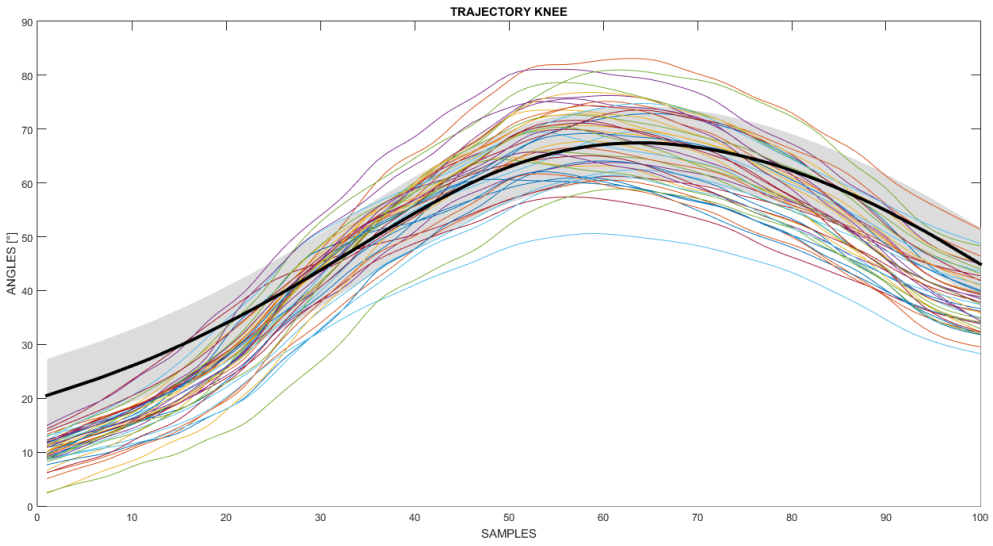

b)

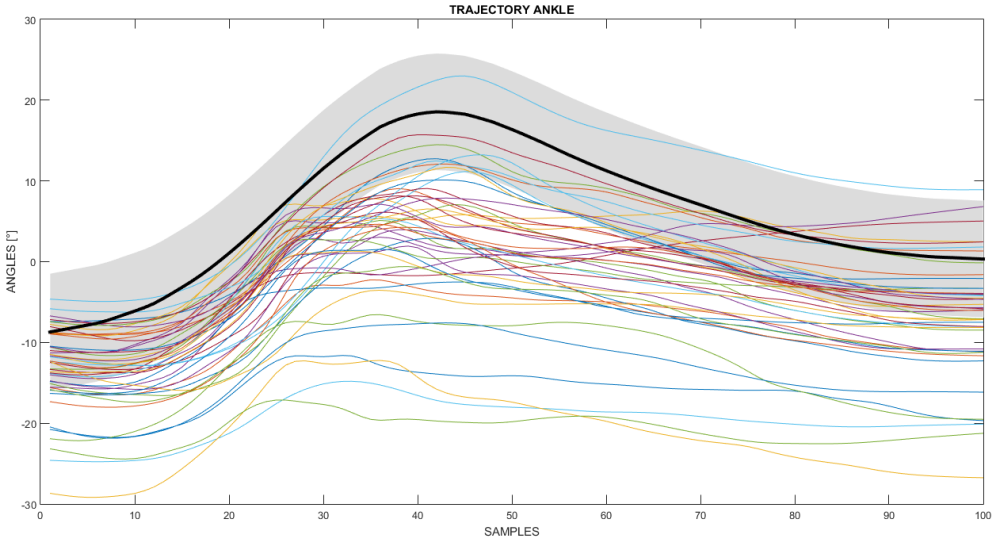

Fig.33. In panel a and panel b are shown the comparisons between references (black lines) of knee and ankle, with their standard deviations (gray), and the trajectories acquired during the different cycles.

Analyzing the comparison between trajectories and references, for both knee and ankle, it can be seen that the results obtained were similar to the angular values of knee and ankle, extracted during the first two tasks. This means that the increasing of stimulation intensity, as shown in figure 34a, was able to correct knee flexion in order to reach physiological values.

Referring to ankle trajectories, values obtained were always lower than the reference, so the distribution of stimulation of the ankle after few steps reached the upper saturation value, as shown in figure 34b.

a)

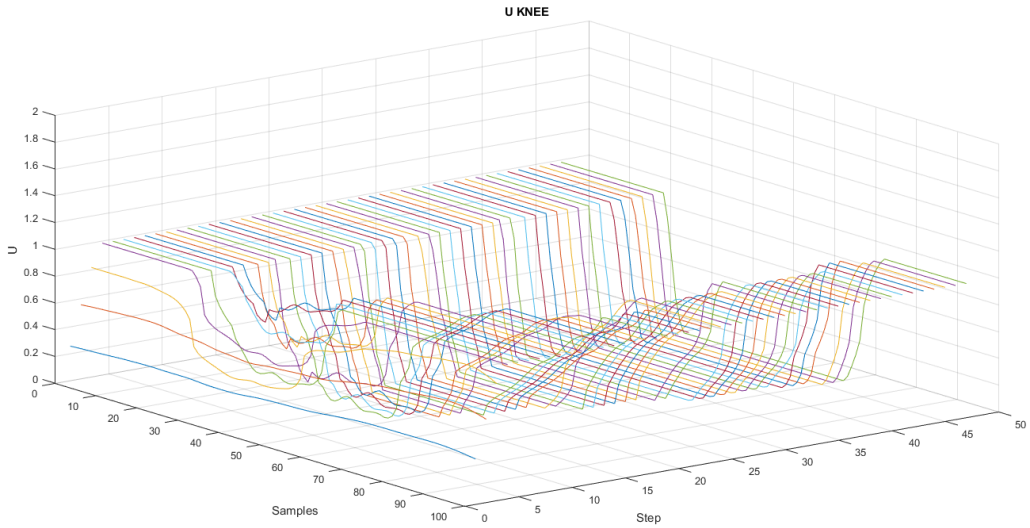

b)

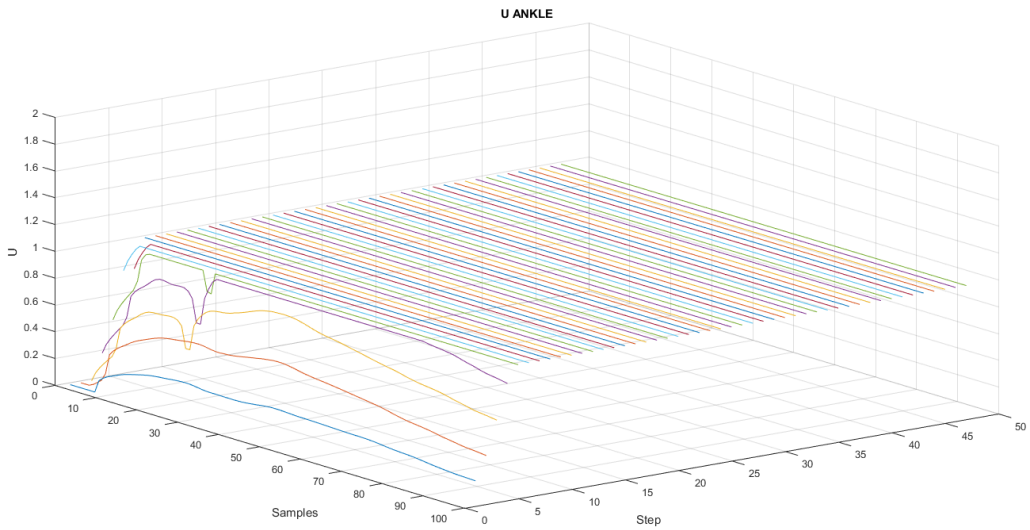

Fig.34. Distribution of stimulation of knee joint (panel a) and ankle joint (panel b)

The results obtained in terms of stimulation profiles are shown in figure 35.

a)

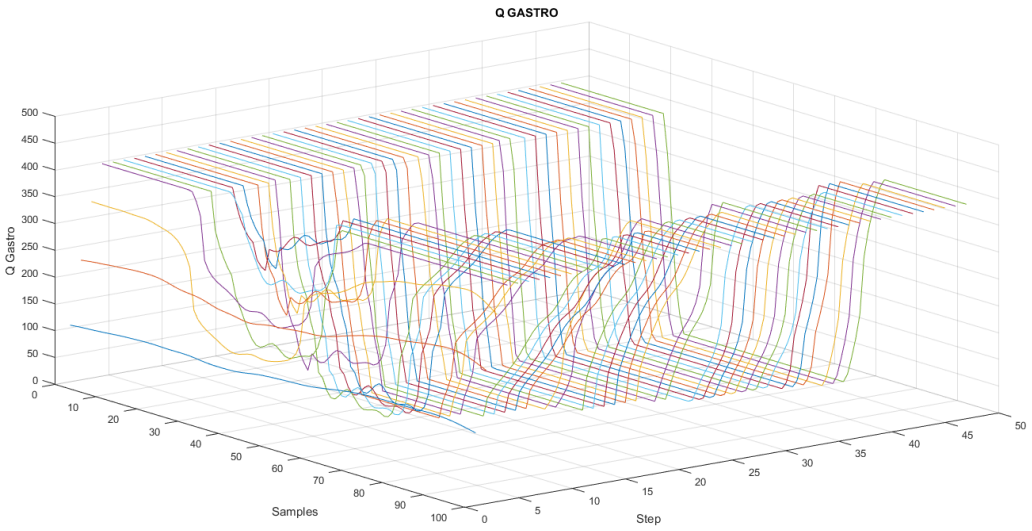

b)

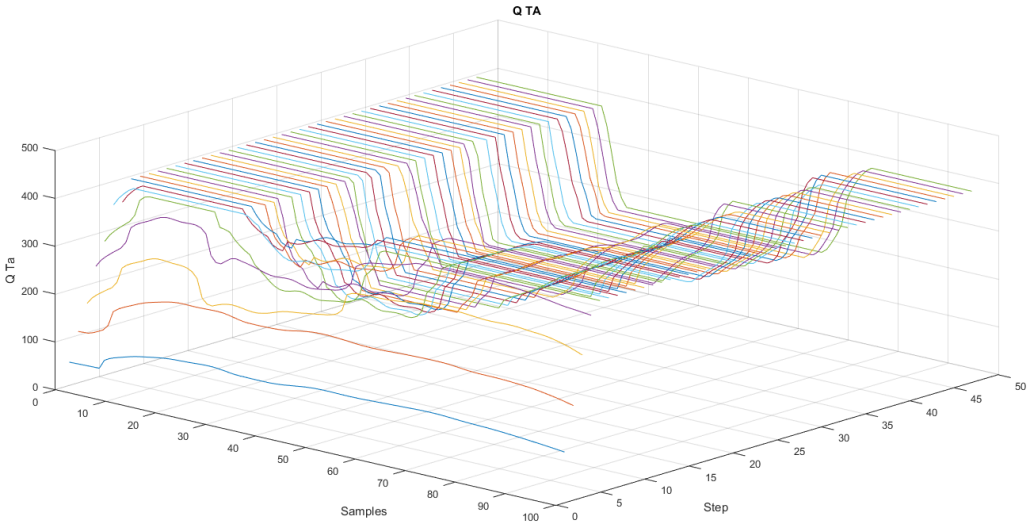

Fig.35. Stimulation profile given to the gastrocnemius (panel a) and to the tibialis anterior (panel b).

The results obtained, in terms of mean values and standard deviations calculated as explained in section 2.2.3, with a one way Anova test, are shown in figure 36.

a)

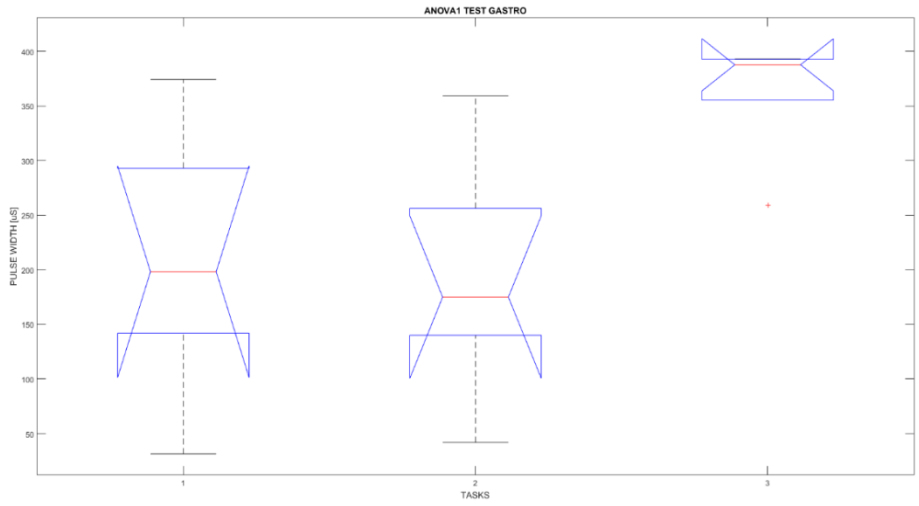

b)

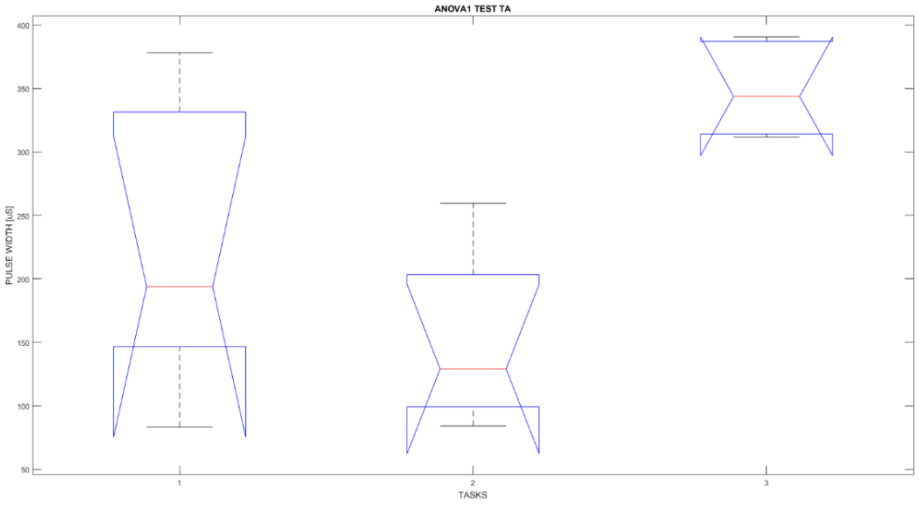

Fig.36. Panel a: a boxplot for each trial regarding the gastrocnemius stimulation is shown, task one corresponds to a normal walking, task 2 correspond to the change in velocity during walking and task 3 refers to walking with a reduced knee flexion. In panel b are shown the same data, calculated for the tibialis anterior.

The mean values of the stimulation profiles, calculated for each task, corresponded to 198.22 μs with a standard deviation of 104.48 μs for the gastrocnemius and 193.84 μs , with a standard deviation of 75.90 μs for the tibialis anterior.

During task 2 the mean values, respectively for the gastrocnemius and the tibialis anterior, were 175.02 μs, with a standard deviation of 128.19 μs, and 129.02 μs, with a standard deviation of 73.30 μs.

During walking with a reduced knee flexion, the values of the parameters were quite different. In fact, referring to the gastrocnemius, the mean value extracted was equal to 387.70 μs, with a standard deviation of 35.50 μs, whereas referring to the tibialis anterior the mean value was 343.80 μs, with a standard deviation of 45.08 μs.

As featured in figure 36, parameters calculated during task 3 were quite different from the parameters computed during the other two trials.

The discussion of these results will be explained in next chapter.

4. Discussion and Conclusion

The results obtained from the separation of the calibration from the original RTD code show that the new version of the segmentation algorithm worked properly. The validation of the algorithm, through which the accuracy of the software was assessed, gave positive results during all the tasks performed. The best results, in terms of metrics P, R and F-1 score were obtained, during the first task performed, walking straight for twenty steps. This result was very important because no FP or FN were found during all the three repetitions of the task, performed by two healthy subjects. Also the other tasks performed gave positive results in terms of accuracy of the algorithm. For this reason the neuroprosthesis was tested in different conditions, such as normal walking, changes in velocity and changes in the pattern of walking.

The gait segmentation started to detect all the gait events from the first step of the trial, which can be an advantage for patients with walking impairments. They can start immediately the walking task in order to increment the useful steps and make more effective the task that could be a rehabilitation program, indeed these subjects could have problems in terms of energy consumption. Another advantage was that in some tasks, the new version of the algorithm worked better compared to the original RTD algorithm, indeed for the start and stop trial, the previous version mismatch the detection of one gait events the subject stopped his walking, whereas the new version detected better the state as shown in figure 19, panel “e”. A possible explanation could be that the thresholds in the old version were not already updated properly while in the new one the calibration parameters were saved in the calibration file and were already updated, so the algorithm worked in right way from the first step of the trial.

Regarding the kinematic section of the algorithm, three methods were considered. The first approach was based on rotation matrices, which was later rejected due to electromagnetic

interferences that corrupted all the data of the magnetometers sensor that were used to extract the orientation matrices of each sensor.

The second approach consisted in the use of gyroscopes and accelerometers present in the IMU sensors. This part was divided into three steps: the first part extracted angles from the accelerometers, the second extracted angles with the gyroscopes and the last part performed an integration of those data. To extract the values of the angle from the accelerometers, the acceleration vector of each segment of the leg in the sagittal plane was extracted, and then the arc cosine of the dot product between two consecutive segment and the angle was calculated. To extract the angles from the gyroscope, the signal was filtered and subsequently integrated in order to obtain an angle. Due to the drift of gyroscope, a possible solution was to took into account the gyroscope data from left double support phase to the mid swing of the right leg and took the accelerometers data during the stance phases due to the relatively low accelerations of the knee and ankle in the stance phase. The results were not so good as expected, since the data were not compatible with the physiological range of motion of the knee joint. Indeed in some cases the angles went down to values around -20 degrees, for these reasons this approach was refused. The last approach used only the gyroscope data to extract the angle trajectories. The problem of the drift in the data was solved performing a detrend algorithm on every single stride during walking. In this case, the angles of knee and ankle were compatible with the physiological range of motion of both joints. One problem of this approach was that the detrend algorithm started to work from the second step and it was highly dependent from the state detection, indeed if there was lack in the detection of one state, the algorithm did not work in the corresponding step and restarted to work on the following step. Although this problem, that could lead to errors during kinematic analysis, and so affect the correct behavior of the neuroprosthesis, the algorithm was chosen to process knee and ankle angles during experimental trials, because the results obtained from the accuracy analysis made with the metrics P, R and F1-score showed that, during the performances of the tasks requested to test the neuroprosthesis (normal walking and changes in velocity), the algorithm was highly reliable in detecting gait

phases. After the kinematic extraction a reference trajectory was obtained using data from twelve healthy young subjects and used to test the robustness of the neuroprosthesis, on seven young healthy subjects. The age of the subjects included in the study was acceptable because the kinematic did not change with the aging of the person. The last part of the work consisted in the development of an ILC to control the neuroprosthesis. Two pairs of stimulation electrodes were used to control the angles of knee and ankle, by placing the electrodes over the gastrocnemius and the tibialis anterior. The first muscle was used to control the knee flexion, whereas the tibialis anterior was used to compensate the plantarflexion of the foot due to the stimulation of the gastrocnemius, keeping the ankle plantarflexion close to the reference. The ILC algorithm calculated the error between a reference trajectory and the actual trajectory, then an intensity distribution (u) was calculated and a stimulation profile (q) was obtained to stimulate the two muscles. To compare the signals extracted from the sensors, a reference trajectory was extracted from healthy subjects, this choice was taken considering also the variability of the SCI subjects, indeed a trajectory of ankle and knee in a patient was different from the healthy people, as shown in figure 37.

a)

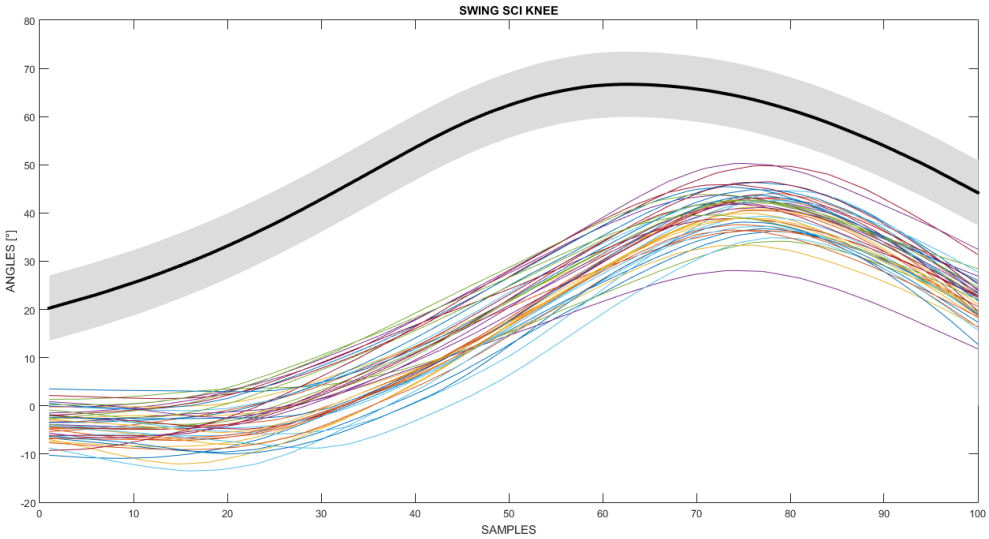

b)

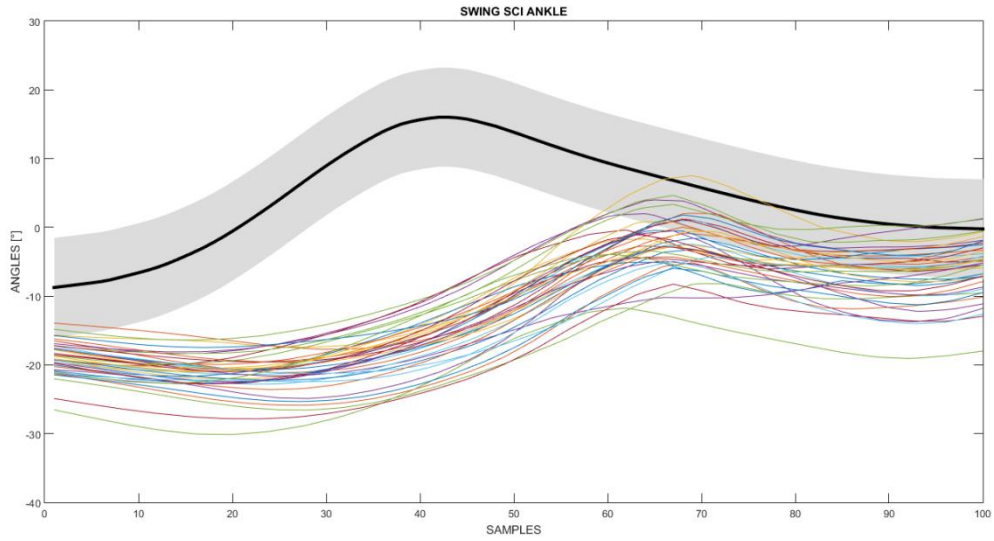

Fig.37. Representation of the swing phases of a SCI subject in a normal walking trial. In panel (a) is displayed the healthy reference of the knee angles with the respectively variability while in panel (b) is represented the healthy reference of the ankle angles with the respectively variability.

All the trajectories obtained from the patients were calculated in the same way as for the healthy subjects. The pathological subjects were under the healthy reference. Thus, to solve this problem a possible solution was to stimulate the muscles that provided an increment of knee and ankle flexion.

To establish a range of normality around the reference trajectory, not only the mean trajectory was extracted from the healthy joint-angle dataset, but also its standard deviation. The reference was used to calculate the error, if the trajectory is greater than the reference the stimulation was reduced. If the current trajectory of the subject was between the value of reference ± the value of standard deviation, λ was reduced in order to avoid an over-damped system, so the variation of the intensity of stimulation was reduced. This was done in order to avoid continuous changing in stimulation of the muscles in which the fatigue could overcame quickly, reducing the efficacy of the neuroprosthesis.

Another method used to avoid a useless stimulation of the muscle was to calculate a mean error over the last five steps of the trial. If the current kinematics were below the reference angle, if the error over the last five steps had not been reduced by 10%, the stimulation was kept constant. Otherwise, the control variable was increased and a profile stimulation was calculated. This type of control allowed to stimulate mostly the muscles if the subject was under the reference trajectory, while at the same time reduce the stimulation if the subject had a healthy stride. The stimulation was maintained constant also when the mean error was kept constant, to avoid useless stimulation. Indeed, if the error did not change for five steps it means that the stimulation did not improve the angular trajectory so it was not necessary to stimulate with a higher pulse width.

The pulse width that was chosen for the stimuli was initially set to 200 μs, but after some experimental trials this value was changed to 400 μs in order to allow trials with lower current amplitudes, with a similar amount of electric charge. The stimulation frequency was set to 25 Hz to avoid the presence of twitches during the muscles contraction.

From the analysis of the control variable (u), it raised that in all the trials of the majority of the subjects involved in the study, the u ankle it was always saturated to the maximum value, due to this the minimum pulse width of the tibialis anterior it was always equal or greater than 200 μs.

A possible explanation was that the current saved during the calibration phase was too low to correct the trajectory of the ankle angle, this could be due to wrong positioning of the electrodes. Indeed if the electrodes placed on tibialis anterior were positioned in the wrong way the ankle could be subjected to an eversion or an inversion as well as a flexion. Another aspect that has to be take into account is that the reference of the ankle was not suitable for all the subjects in the same way because the ankle joint has more degrees of freedom respect to the knee joint.

Another aspect that had to be taken into account was the delay that occurred during FES, in literature was found that the delay in stimulation could vary from 27 ms [21] to 500 ms [22], in this work the delay was set to 150 ms, in the middle of the two literature values. From a

direct response of the subjects involved in the trials the timing of the stimulation was compatible with the gait In a future application of the neuroprosthesis this time could be calculated ad hoc for each subject after a preliminary trial.

The final application of the neuroprosthesis has to be done on incomplete SCI subjects able to walk alone or with walking aids. Otherwise, the stimulation pulse has to be very high in order to move the leg and fatigue occurs very quickly in the muscles. Another aspect that has to be taken into account is that if the subject is not able to walk alone, the stimulation has to be delivered to more muscles and a walking aid has to be given to the subject in order to guarantee the stability and the safety of the subject, for these patients the neuroprosthesis could be used in order to generate a smooth walking more similar to a healthy one.

The main goal of the work was the implementation of a neuroprosthesis for SCI subjects capable to control the flexion of the knee and dorsiflexion of the ankle during the swing phases. A set of inertial sensors was used in order to extract kinematic and gait phases and a FES system was used to deliver electrical stimulation on the leg, for the flexion of the knee the target muscle was the gastrocnemius and for the dorsiflexion of the ankle was stimulated the tibialis anterior muscle.

The neuroprosthesis was divided into three parts, a first one concerned in the optimization of an existing algorithm that performed a gait-events detection, the work consist in the separation of the calibration code from the entire code in order to perform the calibration only at the beginning of the session.

The second part of the neuroprosthesis referred to the kinematic analysis, three different algorithms were created, one based on the rotation matrices, another one was based on the combination of accelerometers and gyroscopes data in order to extract knee and ankle angles and the last method was based only on gyroscopes data elaborated with a detrend algorithm.

The third part of the neuroprosthesis was the development of the control system. An ILC was used to control knee and ankle flexion. First of all a reference trajectory was calculated from 12 healthy subjects. The error, calculated as the cubic square of the reference minus the

“actual” trajectory, was used to generate the correct stimulation profile that was delivered to the target muscles.

To test the robustness of the algorithm, seven healthy subjects, age 26.28 ± 1.58 years, height of 178.57 ± 12.37 cm, performed three different task, a normal walking trial , a normal walking introducing change in velocities and the last trial consisted in a walking without knee and ankle flexion. The results obtained from the Anova test showed that mean value of stimulation profile computed during the third task, were statistically different for the profiles computed during the other two tasks, with a p-value equal to 0.015 for the gastrocnemius and 0.0019 for the tibialis anterior. From the analysis of these values could be inferred that the neuroprosthesis was capable to adapt the values of the stimulation profile in order improve knee and ankle trajectories, during trials in which the subjects walked with a reduced knee flexion, whereas, in case of normal walking, with a constant velocity or with changes in velocity, there were no statistically differences. In fact the stimulation profiles assumed mean values quite low at every step and similar during the performance of the two tasks.

The results obtained shown that the algorithm was capable to adapt to all tasks performed.

Some possible future developments could be the extension of test group with a large number of healthy subjects with different ages and also extend the experimental trials on SCI subjects. Another possible step may be to test the neuroprosthesis on different tasks that can occur in normal life, such as circle walking, stop during walking, changes in slope, walking on stairs.

Bibliography

[1] Lawrence S Chin, “Spinal Cord Injuries: Practice Essentials, Background, Anatomy,” Nov. 2015.

[2] A. J. Bergquist, J. M. Clair, O. Lagerquist, C. S. Mang, Y. Okuma, and D. F. Collins, “Neuromuscular electrical stimulation: implications of the electrically evoked sensory volley,” *Eur. J. Appl. Physiol.*, vol. 111, no. 10, pp. 2409–2426, Oct. 2011.

[3] N. Chia Bejarano, E. Ambrosini, A. Pedrocchi, G. Ferrigno, M. Monticone, and S. Ferrante, “A Novel Adaptive, Real-Time Algorithm to Detect Gait Events From Wearable Sensors,” *IEEE Trans. Neural Syst. Rehabil. Eng.*, vol. 23, no. 3, pp. 413–422, May 2015.

[4] Michael Saulino, “Rehabilitation of Persons With Spinal Cord Injuries: Overview, Common Medical Problems, Thromboembolic Disease,” Sep. 2015.

[5] E. J. Nightingale, J. Raymond, J. W. Middleton, J. Crosbie, and G. M. Davis, “Benefits of FES gait in a spinal cord injured population,” *Spinal Cord*, vol. 45, no. 10, pp. 646–657, Jul. 2007.

[6] http://www.centropiaggio.unipi.it/sites/default/files/course/material/16.%20FES_0.pdf, “Dispensa FES.” .

[7] Manuela Galli, “Dispense del corso di studi ‘Valutazione Funzionale e Riabilitazione Motoria.’” .

[8] V. K. Mushahwar, P. L. Jacobs, R. A. Normann, R. J. Triolo, and N. Kleitman, “New functional electrical stimulation approaches to standing and walking,” *J. Neural Eng.*, vol. 4, no. 3, p. S181, 2007.

[9] L. R. Sheffler and J. Chae, “Neuromuscular electrical stimulation in neurorehabilitation,” *Muscle Nerve*, vol. 35, no. 5, pp. 562–590, May 2007.

[10] T. A. Thrasher, H. M. Flett, and M. R. Popovic, “Gait training regimen for incomplete spinal cord injury using functional electrical stimulation,” *Spinal Cord*, vol. 44, no. 6, pp. 357–361, Oct. 2005.

[11] L. R. Sheffler, M. T. Hennessey, J. S. Knutson, and J. Chae, “Neuroprosthetic effect of peroneal nerve stimulation in multiple sclerosis: a preliminary study,” *Arch. Phys. Med. Rehabil.*, vol. 90, no. 2, pp. 362–365, Feb. 2009.

[12] S. Agarwal, R. J. Triolo, R. Kobetic, M. Miller, C. Bieri, S. Kukke, L. Rohde, and J. A. Davis, “Long-term user perceptions of an implanted neuroprosthesis for exercise, standing, and transfers after spinal cord injury,” *J. Rehabil. Res. Dev.*, vol. 40, no. 3, pp. 241–252, Jun. 2003.

[13] J. L. Collinger, S. Foldes, T. M. Bruns, B. Wodlinger, R. Gaunt, and D. J. Weber, “Neuroprosthetic technology for individuals with spinal cord injury,” *J. Spinal Cord Med.*, vol. 36, no. 4, pp. 258–272, Jul. 2013.

[14] Alessandra Pedrocchi, “NeuralControllers_for_FES_nov102011_LEZ10.pdf.” .

[15] M. Ferrarin, F. Palazzo, R. Riener, and J. Quintern, “Model-based control of FES-induced single joint movements,” *IEEE Trans. Neural Syst. Rehabil. Eng.*, vol. 9, no. 3, pp. 245–257, Sep. 2001.
[16] K. Kurosawa, R. Futami, T. Watanabe, and N. Hoshimiya, “Joint angle control by FES using a feedback error learning controller,” *IEEE Trans. Neural Syst. Rehabil. Eng.*, vol. 13, no. 3, pp. 359–371, Sep. 2005.
[17] Technaid, *Techanid DataSheet*. .
[18] X-Sens, “MTi and MTx User Manual and Technical Documentation.pdf.” .
[19] G. T. David Eberly, “Euler Angle Formulas.”
[20] T. Seel, D. Laidig, M. Valtin, C. Werner, J. Raisch, and T. Schauer, “Feedback control of foot eversion in the adaptive peroneal stimulator,” in *2014 22nd Mediterranean Conference of Control and Automation (MED)*, 2014, pp. 1482–1487.
[21] C.T. Freeman, “Iterative learning control of FES applied to the upper extremity for rehabilitation.” .
[22] C T Freeman, “Phase-lead iterative learning control algorithms.pdf.” .